Journal of Statistical Physics, Vol. 105, Nos. 1/2, October 2001 (© 2001)

Density Profiles in a Classical Coulomb Fluid Near a Dielectric Wall. II. Weak-Coupling Systematic Expansions

Jean-Noël Aqua[1] **and Françoise Cornu**[1]

Received November 14, 2000; revised May 11, 2001

In the framework of the grand-canonical ensemble of statistical mechanics, we give an exact diagrammatic representation of the density profiles in a classical multicomponent plasma near a dielectric wall. By a reorganization of Mayer diagrams for the fugacity expansions of the densities, we exhibit how the long-range of both the self-energy and pair interaction are exponentially screened at large distances from the wall. However, the self-energy due to Coulomb interaction with images still diverges in the vicinity of the dielectric wall and the variation of the density is drastically different at short or large distances from the wall. This variation is involved in the inhomogeneous Debye–Hückel equation obeyed by the screened pair potential. Then the main difficulty lies in the determination of the latter potential at every distance. We solve this problem by devising a systematic expansion with respect to the ratio of the fundamental length scales involved in the two coulombic effects at stake. (The application of this method to a plasma confined between two ideally conducting plates and to a quantum plasma will be presented elsewhere). As a result we derive the exact analytical perturbative expressions for the density profiles up to first order in the coupling between charges. The mean-field approach displayed in Paper I is then justified.

KEY WORDS: Coulomb interactions; dielectric wall; grand-canonical ensemble; systematic resummations; inhomogeneous Debye–Hückel equation; screened potential with two characteristic length scales.

[1] Laboratoire de Physique Théorique, Bâtiment 210, Université Paris-Sud, 91405 Orsay Cedex, France. Laboratoire associé au Centre National de la Recherche Scientifique, UMR 8627.

0022-4715/01/1000-0245$19.50/0 © 2001 Plenum Publishing Corporation

1. INTRODUCTION

The present paper is devoted to the systematic derivation of the density profiles which are discussed in Paper I. The system is a classical multicomponent plasma, made of at least two species of moving charges with opposite signs, near a plane wall macroscopically characterized by a dielectric constant. The exact analytic expressions are obtained in the limit of weak Coulomb coupling inside the fluid.

Our calculations performed in the framework of statistical mechanics cast a new light on the fundamental phenomenon in such systems: Coulomb screening of surface polarization charges inside the fluid. Indeed, from electrostatics it is well known that the bulk thermodynamic properties in a fluid of charges are independent from the charge state of boundary walls. Nevertheless the microscopic long-ranged Coulomb pair interaction $v(\mathbf{r};\mathbf{r}')$ between two unit charges located respectively at $\mathbf{r}$ and $\mathbf{r}'$ takes into account the electrostatic response of the wall: $v(\mathbf{r};\mathbf{r}')$ is a solution of Poisson equation

$$\Delta_{\mathbf{r}'} v(\mathbf{r};\mathbf{r}') = -4\pi\delta(\mathbf{r}-\mathbf{r}') \tag{1.1}$$

and its expression is ruled by the electrostatic boundary conditions. For instance, when the material of the wall is characterized by a relative dielectric constant ϵ_w (with respect to the dielectric constant in the vacuum), the solution of (1.1) reads

$$v_w(\mathbf{r};\mathbf{r}') = \frac{1}{|\mathbf{r}-\mathbf{r}'|} - \Delta_{el}\frac{1}{|\mathbf{r}-\mathbf{r}'^*|} \tag{1.2}$$

where $\Delta_{el} \equiv (\epsilon_w - 1)/(\epsilon_w + 1)$ and $\mathbf{r}'^*$ is the image of $\mathbf{r}'$ with respect to the plane interface.[7] On the contrary, far away from any boundary or when the wall has no electrostatic response ($\epsilon_w = 1$) the potential takes its "bulk" value,

$$v_B(\mathbf{r};\mathbf{r}') = \frac{1}{|\mathbf{r}-\mathbf{r}'|} \tag{1.3}$$

Short-distance cut-offs must be introduced in order to prevent the collapse between charges with opposite signs or between every charge and its image when $\epsilon_w > 1$.

At the inverse temperature $\beta = 1/k_B T$, where k_B is Boltzmann constant, the four length scales in the problem are: the closest approach distance βe^2 determined by Coulomb interaction between charges of typical magnitude e and with a mean kinetic energy of order $1/\beta$; the mean interparticle

distance a; the range b of the hard-core repulsion from the wall (which is chosen to be the same for all species); the hard-core diameter σ of charges which prevents the electrostatic collapse inside the fluid. However the cut-off σ proves not to arise in the densities and correlations at leading order in a low-density regime (because the long range of Coulomb interactions is then the most important effect).

In the grand canonical ensemble (Section 2) the macroscopic parameters are the volume of the system, the fugacities z_α's, where α is a species index running from 1 to the number of species n_s, and the inverse temperature β. The task of getting exact analytic results for a multicomponent plasma where a cut-off is added, and where the screening of the long-range part of the interaction is systematically dealt with, was achieved for the density expansion of bulk correlations by Meeron.[11] Haga extended Meeron's scheme to the low-density expansion of the pressure[5] in the bulk where densities are uniform.[2]

In Section 3 we devise a new reorganization of Mayer fugacity-expansions for every particle density $\rho_\alpha(x; \{z_\gamma\}, \beta)$ and its uniform bulk limit $\rho_\alpha^{\mathrm{B}}(\{z_\gamma\}, \beta)$ in order to exactly deal with the long range of the self-energy of a charge interacting with its image inside the wall as well as with the long range of Coulomb pair interactions. (x is the distance from the plane wall located at $x = 0$. The notations $\{z_\gamma\}$ means that the fugacities of all species are involved.) Our reorganization of diagrams is performed in two steps. In the first step we exhibit how the screening of the bare one-body interaction with the dielectric wall may be described by resummations of "ring" subdiagrams. In the second step, we use an already known method in order to exactly handle with the screening of Coulomb pair interactions.[2] (We notice that, if we had used a one-step resummation analogous to that performed in refs. 1 or 2, there would have been resummed diagramms with some bare self-energies left—and therefore some spurious $1/x$ tails left—which would disappear only by an adequate gathering with other diagrams to be specified in every particular case.)

The latter exact systematic resummations produce auxiliary screened potentials ϕ_1 and ϕ_2 each of which obeys a second-order differential equation studied in Section 4. The technical difficulty lies in the resolution of these auxiliary inhomogeneous Debye–Hückel equations.

In order to get explicit analytic expressions, we consider a regime of weak coupling inside the fluid

$$\Gamma \equiv \frac{\beta e^2}{a} \ll 1. \tag{1.4}$$

[2] Apart from a minor error in the calculation of the coefficient called S_2, his result is correct.

However, the electrostatic coupling with the dielectric wall is not necessarily weak even in the very vicinity of the wall,

$$\frac{\beta e^2}{b} \sim 1 \tag{1.5}$$

After resummation of coulombic long-range divergencies, collective screening effects operate on a scale equal to the bulk Debye length, κ_D^{-1}, with

$$\kappa_D \equiv \sqrt{4\pi\beta \sum_\alpha e_\alpha^2 \rho_\alpha^{\mathrm{B}}} \propto \frac{\Gamma^{\frac{1}{2}}}{a} \tag{1.6}$$

The weak-coupling condition (1.4) is equivalent to the condition

$$a^2 \ll \kappa_D^{-2} \tag{1.7}$$

At the same time, the density profile proves to be an expansion in integer powers—possibly multiplied by some powers of logarithms—not of the coupling parameter $\beta e^2/a = \Gamma$ but of

$$\varepsilon_D \equiv \tfrac{1}{2}\beta e^2 \kappa_D \propto \Gamma^{3/2} \ll 1 \tag{1.8}$$

Thus an ε_D-expansion provides an expansion in powers of the square root of the density. (The cut-off σ for pair interactions corresponds to an integrable interaction; so it arises in the corrections to bulk quantities only from the relative order proportional to the density, namely from the order ε_D^2.)

We show that the screened potentials ϕ_1 and ϕ_2 can be expanded in powers of the ratio $\tilde{\lambda}$ of the two length scales βe^2 and κ_D^{-1} which controls the variations of the x-dependent inverse Debye length in the equation obeyed by each ϕ_i. The expansion of each $\phi_i(\mathbf{r}, \mathbf{r}')$ is uniform with respect to the distances x and x' from the wall—when the projection of $\mathbf{r}-\mathbf{r}'$ onto the wall is kept fixed—in the sense that the term of order $\tilde{\lambda}^n$ is bounded for all $x > b$ and $x' > b$ by a constant which depends on $\kappa_D b$ and $\tilde{\lambda}/[\kappa_D b] = \beta e^2/b$. In fact $\tilde{\lambda}$ coincides with ε_D in the present problem and a scaling analysis of Mayer diagrams allows one to obtain the small-ε_D expansion of the density profile (see Section 5). Only one diagram contributes up to first order in ε_D and $\rho_\alpha(x; \{z_\gamma\}, \beta)$ can be explicitly rewritten as $\rho_\alpha(x; \{\rho_\gamma^{\mathrm{B}}\}, \beta)$. The latter general scheme, which provides systematic expansions in $\tilde{\lambda}$ and ε_D, can be also applied to a classical plasma near a charged dielectric or an ideally conducting wall or to a low-degenerated

quantum plasma in the vicinity of a boundary with any electrostatic response. The corresponding works will be displayed elsewhere.

Eventually, at first order in the coupling parameter ε_D,

$$\rho_\alpha(x) = \rho_\alpha^{\mathrm{B}}\theta(x-b)\exp\left[\Delta_{\mathrm{el}}\beta e_\alpha^2\frac{e^{-2\kappa_D x}}{4x}\right]\times[1+R(\kappa_D x;\varepsilon_D,\kappa_D b)] \tag{1.9}$$

where R is of order $\varepsilon_D \ln \varepsilon_D$ and ε_D. $R(\kappa_D x)$ decays exponentially fast at large distances over the scale κ_D^{-1} and tends to a finite value when x comes to zero. Subsequently, $\rho_\alpha(x)$ varies drastically over the bare-coupling scale βe^2 very close to the wall, whereas its variation at distances larger than κ_D^{-1} is scaled by the screening length κ_D^{-1}. In other words, very near the wall, $\rho_\alpha(x)$ is governed by the part of the self-energy of each particle originating from the electrostatic response of the dielectric wall, whereas the mean Coulomb interaction with other charges of the fluid modified by the impenetrable wall dominates the approach to the bulk value far away from the wall. After calculation of the electrostatic potential drop $\Phi(x)$ at leading order ε_D from the charge density profiles given by (1.9), the density profiles prove to coincide with the expressions derived from the mean-field approach introduced in Paper I,

$$\rho_\alpha(x) = \rho_\alpha^{\mathrm{B}}\theta(x-b)\, e^{-\beta e_\alpha^2 V_{\mathrm{self}}^{sc}(x)}[1-\beta e_\alpha\Phi(x)] \tag{1.10}$$

where $V_{\mathrm{self}}^{sc}(x)$ is the screened self-energy at order ε_D arising from the first step in the resummations of Mayer diagrams.

2. MODEL

2.1. Potential Energy

The total potential energy is the sum of the electrostatic energy U_{elect} and the short-range repulsive interaction U_{SR}. U_{elect} is equal to the sum of Coulomb pair interactions plus the sum of self-energies in the presence of the wall,

$$U_{\mathrm{elect}} = \tfrac{1}{2}\sum_{i\neq j} e_{\alpha_i}e_{\alpha_j}v_{\mathrm{w}}(\mathbf{r}_i;\mathbf{r}_j) + \sum_i e_{\alpha_i}^2 V_{\mathrm{self}}(x_i) \tag{2.1}$$

In (2.1) e_{α_i} is the charge of particle i and

$$V_{\mathrm{self}}(x_i) = -\Delta_{\mathrm{el}}\frac{1}{4x_i} \tag{2.2}$$

where $\Delta_{\rm el}$ is defined in (1.2).[9] The repulsion energy $U_{\rm SR}$ is also the sum of hard-core pair interactions plus the sum of one-body potentials created by the wall,

$$U_{\rm SR} = \tfrac{1}{2} \sum_{i \neq j} v_{\rm SR}(\mathbf{r}_i - \mathbf{r}_j) + \sum_i V_{\rm SR}(x_i) \tag{2.3}$$

with

$$\exp[-\beta v_{\rm SR}(\mathbf{r}_i; \mathbf{r}_j)] = \begin{cases} 0 & \text{if} \quad |\mathbf{r}_i - \mathbf{r}_j| < \sigma \\ 1 & \text{if} \quad |\mathbf{r}_i - \mathbf{r}_j| > \sigma \end{cases} \tag{2.4}$$

and

$$\exp[-\beta V_{\rm SR}(x)] = \begin{cases} 0 & \text{if} \quad x < b \\ 1 & \text{if} \quad x > b \end{cases} \tag{2.5}$$

We notice that in the case $\epsilon_{\rm w} < 1$, $\exp(-\beta e_\alpha^2 V_{\rm self}(x))$ vanishes when x goes to zero and $V_{\rm SR}$ can be omitted, i.e., b can be set to zero, without any collapse of the system onto the wall.

2.2. Fugacity Expansions

The grand partition function of the system in the semi-infinite space $x > 0$ reads

$$\Xi(\beta, \{z_\gamma\}) = \sum_{N=0}^{+\infty} \frac{1}{N!} \int \left[\prod_{i=1}^{N} d\mathscr{P}_i \, z_{\alpha_i} \right] e^{-\beta(U_{\rm elect} + U_{\rm SR})} \tag{2.6}$$

In (2.6) the integration measure is denoted by $\int d\mathscr{P}_i \equiv \int_{x_i > 0} d\mathbf{r}_i \sum_{\alpha_i = 1}^{n_s}$ and $\mathscr{P}_i$ is the notation for $(\mathbf{r}_i, \alpha_i)$. z_{α_i} has the dimension of an inverse cubed distance. The one-body interactions can be absorbed in an x-dependent fugacity

$$\bar{z}_{\alpha_i}(x_i) \equiv z_{\alpha_i} e^{-\beta[V_{\rm SR}(x_i) + e_{\alpha_i}^2 V_{\rm self}(x_i)]} \tag{2.7}$$

According to (2.2) and (2.5)

$$\bar{z}_{\alpha_i}(x_i) = z_{\alpha_i} \theta(x_i - b) \, e^{\Delta_{\rm el} \beta e_{\alpha_i}^2 / (4x_i)} \tag{2.8}$$

where θ is the Heaviside function. Ξ can be written as

$$\Xi(\beta, \{z_\gamma\}) = \sum_{N=0}^{+\infty} \frac{1}{N!} \int \left[\prod_{i=1}^{N} d\mathscr{P}_i \, \bar{z}_{\alpha_i}(x_i) \right] e^{-\frac{\beta}{2} \sum_{i \neq j} [v_{SR}(\mathbf{r}_i - \mathbf{r}_j) + e_{\alpha_i} e_{\alpha_j} v_w(\mathbf{r}_i; \mathbf{r}_j)]} \tag{2.9}$$

The particle density for species α is derived from the grand partition function through a functional derivative

$$\rho_\alpha(x; \beta, \{z_\gamma\}) = \bar{z}_\alpha(x) \frac{\delta \ln \Xi(\beta, \{z_\gamma^*\})}{\delta z_\alpha^*(x)} \bigg|_{z_\alpha^*(x) = \bar{z}_\alpha(x)} \tag{2.10}$$

By definition of the bulk

$$\lim_{x \to +\infty} \rho_\alpha(x; \beta, \{z_\gamma\}) = \rho_\alpha^B(\beta, \{z_\gamma\}) \tag{2.11}$$

According to the survey of the existence of thermodynamic limit for Coulomb fluids,[10] the bulk densities satisfy the local neutrality

$$\sum_\alpha e_\alpha \rho_\alpha^B(\beta, \{z_\gamma\}) = 0 \tag{2.12}$$

whatever the values of the z_γ's are. In the following we will consider a weak coupling regime where the system behaves as an ideal gas at zeroth order in Γ. Besides, the particle density of species α in an ideal gas is just proportional to the fugacity z_α. As a consequence, we can take advantage of the freedom of choice for the z_γ's exhibited in ref. 10 and enforce the extra condition

$$\sum_\gamma e_\gamma z_\gamma = 0 \tag{2.13}$$

(2.13) ensures that the ideal gas also satisfies (2.12) and this provides a convenient simplification in the relation between the ρ_γ's and the z_γ's. We stress that the irrelevance of the value taken by one among the fugacities, which is always valid for bulk quantities, also holds for surface statistical properties but only when the wall gets no global influence charge in the presence of the Coulomb fluid. This is indeed the case when ϵ_w is finite. On the contrary, when ϵ_w is sent to infinity, the wall material is an ideal conductor which gains a global charge by influence. The latter is exactly compensated by the net surface charge in the fluid and it depends on all fugacities z_γ's.

2.3. Representation of the Density Profile in Terms of Mayer Diagrams

The fugacity-expansion (2.9) may be expressed in terms of Mayer diagrams where a point is associated with every $\mathscr{P}_i$ and two points are joined by at most one bond

$$f(\mathscr{P}_i, \mathscr{P}_j) = e^{-\beta(v_{SR}(\mathbf{r}_i - \mathbf{r}_j) + e_{\alpha_i} e_{\alpha_j} v_w(\mathbf{r}_i; \mathbf{r}_j))} - 1 \tag{2.14}$$

The relation (2.10) and topological arguments[6] lead to various diagrammatic representations for the fugacity expansion of $\rho_\alpha(x)$. In the following we will use

$$\rho_\alpha(x) = \bar{z}_\alpha(x) \exp\left[\sum_{\mathbb{G}} \frac{1}{S_{\mathbb{G}}} \int \prod_{n=1}^{N} [d\mathscr{P}_n \, \bar{z}_{\alpha_n}(x_n)] \left[\prod f \right]_{\mathbb{G}} \right] \tag{2.15}$$

In (2.15) the sum runs over all the unlabeled and topologically different connected diagrams $\mathbb{G}$ with one root point $\mathscr{P} \equiv (\alpha, \mathbf{r})$ (which is not integrated over) and N internal points ($N = 1, \ldots, \infty$). Moreover the $\mathbb{G}$'s satisfy the extra constraint that the root point $\mathscr{P}$ is not an articulation point. ($\mathscr{P}$ is an articulation point of $\mathbb{G}$ if $\mathbb{G}$ is split into at least two pieces when the point $\mathscr{P}$ is removed.) $[\prod f]_{\mathbb{G}}$ is the product of the f bonds in the diagram $\mathbb{G}$ and $S_{\mathbb{G}}$ is the symmetry factor of $\mathbb{G}$, namely the number of permutations between some internal points $\mathscr{P}_n$ that do not change the product $[\prod f]_{\mathbb{G}}$.

At large distances $v_w(\mathbf{r}_i; \mathbf{r}_j)$ behaves essentially as $1/|\mathbf{r}_i - \mathbf{r}_j|$ and the f bonds (2.14) are not integrable. The divergences in Mayer diagrams $\mathbb{G}$ may be removed by splitting the f bonds into several auxiliary bonds f^* and by performing a reorganization of the diagrams $\mathbb{G}^*$ made with f^* bonds. ($\mathbb{G}^*$ diagrams have the same topological properties as $\mathbb{G}$ diagrams.) The decomposition of f chosen for our purpose is

$$f = f^{cc} + \tfrac{1}{2}[f^{cc}]^2 + f_T \tag{2.16}$$

with

$$f^{cc}(\mathscr{P}_i, \mathscr{P}_j) \equiv -\beta e_{\alpha_i} e_{\alpha_j} v_w(\mathbf{r}_i; \mathbf{r}_j) \tag{2.17}$$

With these definitions f_T is at the border of integrability. The systematic partial resummations of diagrams $\mathbb{G}^*$ are described in next section.

3. EXACT TOPOLOGICAL RESUMMATIONS VALID FOR ANY DENSITY

3.1. Step 1: Screening of the Self-Energy Induced by the Wall

The long-range one-body interaction $e_\alpha^2 V_{\text{self}}(x)$ involved in the fugacity $\bar{z}_\alpha(x)$ turns into a short-range effective interaction when Coulomb "ring" subdiagrams are resummed. We introduce the following definitions. A Coulomb "ring" subdiagram carried by a point $\mathscr{P}$ is either a bond $[f^{cc}]^2/2$ or a chain of bonds f^{cc} whose both ends coincide with $\mathscr{P}$ and which contains at least two intermediate points. The value I_r of the sum of all rings attached to a point $\mathscr{P}$ is equal to

$$I_r(x) = -\tfrac{1}{2}\beta e_\alpha^2[(\phi_1 - v_w)(\mathbf{r};\mathbf{r})] \tag{3.1}$$

where $-\beta e_\alpha^2 \phi_1(\mathbf{r};\mathbf{r}')$ is the sum of chains made of an arbitrary number of bonds f^{cc} between $\mathbf{r}$ and $\mathbf{r}'$ and with intermediate points $\mathscr{P}_i$ weighted by $\bar{z}(\mathscr{P}_i)$. (1/2 is the symmetry factor of a single ring diagram.) By definition

$$-\beta e_\alpha e_{\alpha'} \phi_1(\mathbf{r};\mathbf{r}') = f^{cc}(\mathscr{P};\mathscr{P}') + \sum_{N=1}^{+\infty} \int \left[\prod_{i=1}^{N} d\mathscr{P}_i\, \bar{z}(\mathscr{P}_i)\right] \times f^{cc}(\mathscr{P};\mathscr{P}_1)\, f^{cc}(\mathscr{P}_1;\mathscr{P}_2)\cdots f^{cc}(\mathscr{P}_N;\mathscr{P}') \tag{3.2}$$

According to (2.17), the definition (3.2) of ϕ_1 is equivalent to the integral relation

$$\phi_1(\mathbf{r};\mathbf{r}') = v_w(\mathbf{r};\mathbf{r}') - \beta \sum_\alpha e_\alpha^2 \int d\mathbf{r}''\, \bar{z}_\alpha(x'')\, v_w(\mathbf{r};\mathbf{r}'')\, \phi_1(\mathbf{r}'';\mathbf{r}') \tag{3.3}$$

The sum of an arbitrary number of rings carried by a point $\mathscr{P}$ is equal to $\exp I_r(\mathbf{r})$. (An analogous calculation appears in Section V.B of ref. 1.)

Let us consider all diagrams $\mathbb{G}^*$ (with weight $\bar{z}$) that only differ from a given diagram $\mathbb{G}^{*[0]}$ by one or more Coulomb ring subdiagrams carried by at least one point of $\mathbb{G}^{*[0]}$ (see Fig. 1). Before integration over the internal points of $\mathbb{G}^{*[0]}$, the integral corresponding to such a diagram is equal to the integrand associated with $\mathbb{G}^{*[0]}$ times the contributions from Coulomb rings. As a consequence, if we sum all such diagrams $\mathbb{G}^*$ we get one diagram $\mathbb{G}^{*[1]}$ which has the same points and bonds as $\mathbb{G}^{*[0]}$ except that the weights $\bar{z}$ are replaced by weights

$$\bar{z}^{[1]}(\mathscr{P}) = \bar{z}(\mathscr{P}) \exp[-\tfrac{1}{2}\beta e_\alpha^2(\phi_1 - v_w)(\mathbf{r};\mathbf{r})] \tag{3.4}$$

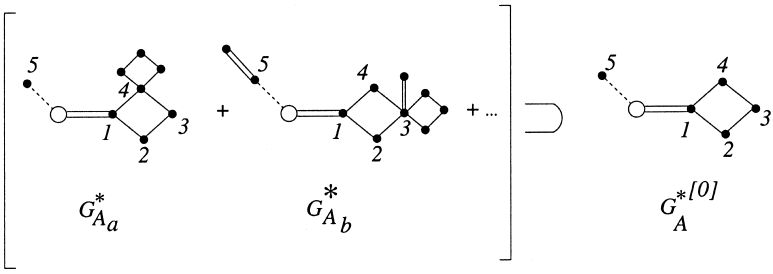

Fig. 1. Step-1 for resummations. G^*_{Aa} and G^*_{Ab} are two diagrams that only differ from $G^{*[0]}_A$ by ring subdiagrams. Labels are attached to points which are common to all diagrams. Each point $\mathscr{P}_i$ carries a weight $\bar{z}(\mathscr{P}_i)$. A bond f^{cc} is drawn as a solid line, a bond $(1/2)[f^{cc}]^2$ as a double solid line and a bond f_T as a dashed line. The subdiagram $\mathbb{S}(\mathscr{P}_1)$ made of points $\mathscr{P}_2$, $\mathscr{P}_3$, $\mathscr{P}_4$ exists in $G^{*[0]}_A$ of Fig. 1 because at least one of the latter points carries a ring in diagrams G^*_{Aa} and G^*_{Ab}.

where $\phi_1(\mathbf{r};\mathbf{r}')$ is defined in (3.2). At the end of the first partial resummation, the diagrams $\mathbb{G}^*$ with bonds f^{cc}, $1/2[f^{cc}]^2$ and f_T and with weights $\bar{z}_\alpha(x)$ have been replaced by diagrams $\mathbb{G}^{*[1]}$ with the same kind of bonds but with weights $\bar{z}^{[1]}_\alpha(x)$ and an extra construction rule $\mathscr{R}$ (see Fig. 2). The latter one is necessary to avoid double counting. If some subdiagram $\mathbb{S}(\mathscr{P}_m)$ of $\mathbb{G}^{*[1]}$ is a ring of bonds f^{cc} with weights $\bar{z}^{[1]}_\alpha$ carried by the point $\mathscr{P}_m$ (with weight $\bar{z}^{[1]}_{\alpha_m}(x_m)$), then after integration over intermediate points in the ring, the contribution from $\mathbb{S}(\mathscr{P}_m)$, which depends only on x_m, is factorized in the total contribution from $\mathbb{G}^{*[1]}$ and is multiplied by the weight $\bar{z}^{[1]}_{\alpha_m}(x_m)$ of its root point $\mathscr{P}_m$; rule $\mathscr{R}$ states that the contribution from $\mathbb{S}(\mathscr{P}_m)$ is equal to its value where all its intermediate points have a weight $\bar{z}^{[1]}_\alpha$ minus the corresponding value where all its intermediate points would have a weight $\bar{z}_\alpha$. Indeed the latter value is already taken into account in the weight

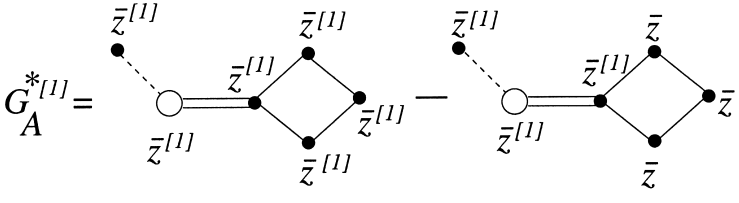

Fig. 2. Example for rule $\mathscr{R}$ after step-1 resummations. After ring summations, G^*_{Aa} and G^*_{Ab} contribute to $G^{*[1]}_A$, whereas the subdiagram $\mathbb{S}(\mathscr{P}_1)$ in $G^{*[0]}_A$ disappears and $G^{*[0]}_A$ contributes to another $G^{*[1]}$. As a result the value of $G^{*[1]}_A$ is equal to an integral where all bonds are the same as in $G^{*[0]}_A$ but where all weights $\bar{z}$ have been replaced by $\bar{z}^{[1]}$ minus the value of the integral corresponding to $G^{*[0]}_A$ where the weights $\bar{z}$ have been replaced by $\bar{z}^{[1]}$ only for points which are not the intermediate points of a ring subdiagram.

$\bar{z}^{[1]}_{\alpha_m}(x_m)$ of the point $\mathscr{P}_m$, whereas a subdiagram of $\mathbb{G}^*$ made of bonds f^{cc} but where at least one intermediate point carries another Coulomb ring does not disappear in the ring resummation process leading to $\mathbb{G}^{*[1]}$. (See Figs. 1 and 2).

According to the definition (2.7) of $\bar{z}(\mathscr{P})$ and since $V_{self}(x) = (1/2)(v_w - v_B)(\mathbf{r}; \mathbf{r})$, (3.4) may be written as

$$\bar{z}^{[1]}_{\alpha}(x) = \theta(x-b)\, z_\alpha \exp[-\tfrac{1}{2}\beta e^2_\alpha (\phi_1 - v_B)(\mathbf{r}; \mathbf{r})] \tag{3.5}$$

As shown below in a weak-coupling expansion, we expect that for any finite coupling constant $(\phi_1 - v_B)(\mathbf{r}; \mathbf{r})$ has no algebraic tail at large distances. Thus, contrary to $\bar{z}_\alpha(x)$ the screened fugacity $\bar{z}^{[1]}_\alpha(x)$ does not contain the long-range part of the self-energy induced by the electrostatic response of the wall when $\epsilon_w \neq 1$. In other words, the resummation of rings subdiagrams has captured the main effect of Coulomb screening upon the electrostatic interaction with the wall.

3.2. Step 2: Screening of Pair Interactions

In the second step we sum all chains of bonds f^{cc} in diagrams $\mathbb{G}^{*[1]}$. The systematic resummation process is performed as follows. We define a "Coulomb" point as the intermediate point of a chain of two bonds f^{cc} and which is not linked to any other point in the diagram. Such a point has a weight $\bar{z}^{[1]}_\alpha$. A so-called "prototype" diagram $\mathbb{P}$ is a diagram $\mathbb{G}^{*[1]}$ which contains no Coulomb point. We sum all diagrams $\mathbb{G}^{*[1]}$ which can be built from the same diagram $\mathbb{P}$ by addition of at least one Coulomb point (with weight $\bar{z}^{[1]}$) with the associated f^{cc} bonds either to replace a f^{cc} bond in $\mathbb{P}$ by a chain of f^{cc} bonds or to multiply a bond in $\mathbb{P}$ (see Fig. 3). In the latter case, we use the convention according to which the diagram $\mathbb{P}$ is the same whether the diagrams $\mathbb{G}^{*[1]}$ contain a bond $(1/2)[f^{cc}]^2(\mathscr{P}_i, \mathscr{P}_j)$ or a bond $f_T(\mathscr{P}_i, \mathscr{P}_j)$ which are possibly multiplied by a chain of f^{cc} bonds between $\mathscr{P}_i$ and $\mathscr{P}_j$. Since the $\mathbb{P}$ diagram may contain articulation points, the resummation produces two effects.

First, we sum all diagrams $\mathbb{G}^{*[1]}$ that differ from $\mathbb{P}$ by a ring of bonds f^{cc} with at least one intermediate point with weight $\bar{z}^{[1]}$. As in the reorganization of diagrams performed in step 1, this process leads to a renormalization of the fugacity by an exponential factor analogous to (3.4) with an extra subtraction arising from the construction rule $\mathscr{R}$ for $\mathbb{G}^{*[1]}$ diagrams. The resummed fugacity reads

$$\bar{z}^{[2]}_\alpha(x) = \bar{z}^{[1]}_\alpha(x) \exp\{-\tfrac{1}{2}\beta e^2_\alpha[(\phi_2 - v_w)(\mathbf{r}; \mathbf{r}) - (\phi_1 - v_w)(\mathbf{r}; \mathbf{r})]\} \tag{3.6}$$

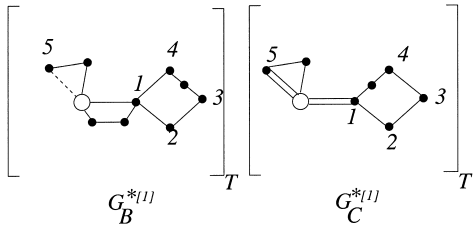

$G_B^{*[1]}$ $G_C^{*[1]}$

Fig. 3. Step-2 for resummations. $G_B^{*[1]}$ and $G_C^{*[1]}$ are two $G^{*[1]}$ diagrams which correspond to the same prototype diagram $\mathbb{P}$ as the diagram $G_A^{*[1]}$ in Fig. 2. The brackets with an index T indicate that the diagrams $G^{*[1]}$ must be calculated with the weights and the subtraction (rule $\mathscr{R}$) displayed in Fig. 2.

where ϕ_2 is defined by the integral equation (3.3) with $\bar{z}_\alpha(x)$ replaced by $\bar{z}_\alpha^{[1]}(x)$. According to (3.4) and (2.8), the expression of $\bar{z}_\alpha^{[2]}(x)$ is similar to (3.5)

$$\bar{z}_\alpha^{[2]}(x) = \theta(x-b)\, z_\alpha \exp[-\tfrac{1}{2}\beta e_\alpha^2(\phi_2 - v_B)(\mathbf{r};\mathbf{r})] \tag{3.7}$$

The second effect of step-2 resummations is a renormalization of the f^* bonds in the final diagrams $\mathbb{P}$. The summation operates for each pair of points in $\mathbb{P}$ independently. (See, for instance, ref. 1 for similar topological considerations.) The sum of all possible single chains made of f^{cc} bonds and whose intermediate points carry weights $\bar{z}^{[1]}$ is

$$F^{cc}(\mathscr{P};\mathscr{P}') = -\beta e_\alpha e_{\alpha'} \phi_2(\mathbf{r};\mathbf{r}') \tag{3.8}$$

The sum of the bond $(1/2)[f^{cc}]^2(\mathscr{P};\mathscr{P}')$ and of all subdiagrams made of the product of a Coulomb chain (possibly made of only one bond $f^{cc}(\mathscr{P};\mathscr{P}')$) and a Coulomb chain with at least one intermediate point linking $\mathscr{P}$ to $\mathscr{P}'$ is merely

$$\tfrac{1}{2}[F^{cc}]^2(\mathscr{P};\mathscr{P}') \tag{3.9}$$

The sum of the bond $f_T(\mathscr{P};\mathscr{P}')$, its product by at least one Coulomb chain with at least one intermediate point, and the product of at least three Coulomb chains, one of which at least contains one intermediate point leads to the simple resummed bond (see refs. 2 and 11)

$$F_{RT} \equiv e^{-\beta v_{SR} + F^{cc}} - 1 - F^{cc} - \tfrac{1}{2}[F^{cc}]^2 \tag{3.10}$$

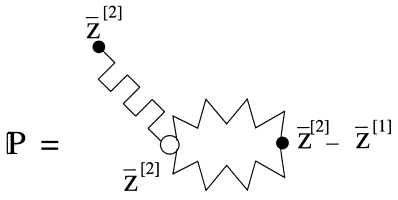

Fig. 4. Diagram $\mathbb{P}$ corresponding to $G_A^{*[1]}$, $G_B^{*[1]}$ and $G_C^{*[1]}$ after step-2 resummation. The crenelated line is a bond F_{RT}, while the double wavyline corresponds to a bond $(1/2)[F^{\mathrm{cc}}]^2$. The rule $\mathscr{R}_2$ is illustrated in the present example.

After resummations the diagrams $\mathbb{P}$ are made of bonds F^{cc}, $(1/2)[F^{\mathrm{cc}}]^2$, and F_{RT} with at most one bond between two points (see Fig. 4) and the following rules. A point—different from the root point—which carries only two bonds F^{cc} has a weight $\bar{z}_\alpha^{[2]} - \bar{z}_\alpha^{[1]}$ ($\mathscr{R}_1$) (see Fig. 5). A point—different from the root point—which is linked only to a $(1/2)[F^{\mathrm{cc}}]^2$ bond has also a weight $\bar{z}_\alpha^{[2]} - \bar{z}_\alpha^{[1]}$ ($\mathscr{R}_2$) (see Fig. 4). The rules $\mathscr{R}_1$ and $\mathscr{R}_2$ arise from the definition of the Coulomb points which disappear in the resummation process and from rule $\mathscr{R}$ of the first step of the resummations. All other points have a weight $\bar{z}_\alpha^{[2]}$. For instance, the diagrammatic representation of $\rho_\alpha(\mathbf{r})$ in terms of $\mathbb{P}$ diagrams starts as

$$\rho_\alpha(\mathbf{r}) = \bar{z}_\alpha^{[2]}(x) \exp\left\{ \sum_\gamma \int d\mathbf{r}'\, \bar{z}_\gamma^{[2]}(x')[F^{\mathrm{cc}} + F_{\mathrm{RT}}](\mathscr{P}; \mathscr{P}') \right.$$
$$\left. + \sum_\gamma \int d\mathbf{r}'\, [\bar{z}_\gamma^{[2]}(x') - \bar{z}_\gamma^{[1]}(x')] \tfrac{1}{2} [F^{\mathrm{cc}}(\mathscr{P}; \mathscr{P}')]^2 + \cdots \right\} \qquad (3.11)$$

The diagrams represented by the dots contain more than one internal point.

4. SCREENED POTENTIALS

4.1. Partial Derivative Equations

The screened potential ϕ_2, as well as the other auxiliary object ϕ_1, are defined through integral equations (3.3). Since v_{w} is a solution of Poisson equation (1.1), (3.3) is equivalent to a set of local equations. For $x' > 0$, the latter ones read

$$\begin{cases} \Delta_{\mathbf{r}} \phi_1(\mathbf{r}; \mathbf{r}') - \overline{\kappa_1}^2(x)\, \phi_1(\mathbf{r}; \mathbf{r}') = -4\pi\delta(\mathbf{r} - \mathbf{r}') & \text{if} \quad x > 0 \\ \Delta_{\mathbf{r}} \phi_1(\mathbf{r}; \mathbf{r}') = 0 & \text{if} \quad x < 0 \end{cases} \qquad (4.1)$$

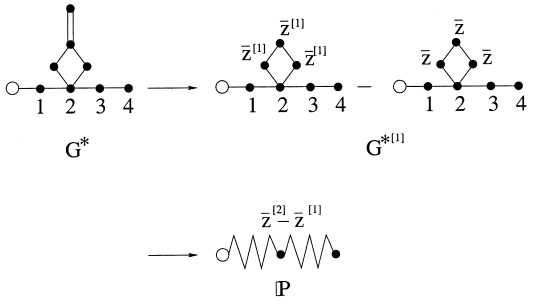

Fig. 5. Example for rule $\mathscr{R}_1$. Diagram G^* contributes to the value of diagram $G^{*[1]}$ after step-1 resummations. The value of $G^{*[1]}$ is determined by rule $\mathscr{R}$. After step-2 resummations $G^{*[1]}$ contributes to diagram $\mathbb{P}$, whose value is given by rule $\mathscr{R}_1$. A single wavy line denotes a bond F^{cc}.

with

$$\overline{\kappa_1}^2(x) \equiv 4\pi\beta \sum_{\alpha} e_\alpha^2 \bar{z}_\alpha(x) \tag{4.2}$$

According to its definition (3.2), ϕ_1 is real. Since the operator $[\Delta_{\mathbf{r}} - \overline{\kappa_1}^2(x)]$ is self-adjoint, the real function $\phi_1(\mathbf{r}; \mathbf{r}')$ is symmetric under exchange of its arguments when $\mathbf{r}$ and $\mathbf{r}'$ are in the same region,

$$\phi_1(\mathbf{r}; \mathbf{r}') = \phi_1(\mathbf{r}'; \mathbf{r}) \tag{4.3}$$

Moreover, the invariance of the system under translations in directions parallel to the plane interface implies that

$$\phi_1(\mathbf{r}; \mathbf{r}') = \phi_1(x, x', \mathbf{y} - \mathbf{y}') \tag{4.4}$$

where $\mathbf{y}$ is the projection of $\mathbf{r}$ onto the plane perpendicular to the x-axis. According to its definition (3.2), ϕ_1 obeys the same boundary conditions as the electrostatic potential v_w: ϕ_1 is continuous in all space,

$$\lim_{x \to 0^-} \epsilon_w \frac{\partial \phi_1}{\partial x}(x, x', \mathbf{y} - \mathbf{y}') = \lim_{x \to 0^+} \frac{\partial \phi_1}{\partial x}(x, x', \mathbf{y} - \mathbf{y}') \tag{4.5}$$

Since $\overline{\kappa_1}^2(x)$ contains a Heaviside distribution at $x=b$ but no Dirac distribution, the derivative of $\phi_1(x, x'; \mathbf{y}-\mathbf{y}')$ is continuous at $x=b$. Moreover $\phi_1(x, x'; \mathbf{y}-\mathbf{y}')$ tends to zero when x goes to $+\infty$ or $-\infty$. All previous properties are also true for $\phi_2(\mathbf{r}; \mathbf{r}')$ with the only difference

$$\overline{\kappa_2}^2(x) \equiv 4\pi\beta \sum_\alpha e_\alpha^2 \bar{z}_\alpha^{[1]}(x) \tag{4.6}$$

4.2. Scaling Property

A Fourier transform allows one to change the system of partial derivative equations (4.1) for each $\phi_j(\mathbf{r}; \mathbf{r}')$ (with $j=1, 2$) into a system of one-dimensional differential equations with respect to x. For $x' > 0$,

$$\left[\frac{\partial^2}{\partial\tilde{x}^2} - (1+\mathbf{q}^2) - U_j(\tilde{x})\right] \tilde{\phi}_j(\tilde{x}, \tilde{x}', \mathbf{q}) = -4\pi\delta(\tilde{x}-\tilde{x}') \quad \text{if} \quad b < x \tag{4.7a}$$

$$\left[\frac{\partial^2}{\partial\tilde{x}^2} - \mathbf{q}^2\right] \tilde{\phi}_j(\tilde{x}, \tilde{x}', \mathbf{q}) = -4\pi\delta(\tilde{x}-\tilde{x}') \quad \text{if} \quad 0 < x < b \tag{4.7b}$$

$$\left[\frac{\partial^2}{\partial\tilde{x}^2} - \mathbf{q}^2\right] \tilde{\phi}_j(\tilde{x}, \tilde{x}', \mathbf{q}) = 0 \quad \text{if} \quad x < 0 \tag{4.7c}$$

In (4.7) we have introduced the dimensionless variable $\tilde{x} = \kappa_j x$ with

$$\kappa_1 \equiv \sqrt{4\pi\beta \sum_\alpha e_\alpha^2 z_\alpha} \tag{4.8}$$

$$\kappa_2 \equiv \sqrt{4\pi\beta \sum_\alpha e_\alpha^2 z_\alpha e^{\varepsilon_\alpha}} \tag{4.9}$$

$$\varepsilon_\alpha \equiv \tfrac{1}{2}\beta e_\alpha^2 \kappa_1 \tag{4.10}$$

and the dimensionless Fourier transform

$$\tilde{\phi}_j(\tilde{x}, \tilde{x}', \mathbf{q}) = \kappa_j \phi_j(x, x', \kappa_j \mathbf{q}) \tag{4.11}$$

with $\phi_j(x, x', \kappa_j\mathbf{q}) \equiv \int d\mathbf{y} \exp[i\kappa_j \mathbf{q}.\mathbf{y}]\, \phi_j(x, x', \mathbf{y})$. According to (2.8) and (4.2), for $\tilde{x} = \kappa_1 x$

$$U_1(\tilde{x}) = \frac{4\pi\beta}{\kappa_1^2} \sum_\alpha e_\alpha^2 z_\alpha (e^{\Delta_{el}\varepsilon_\alpha/(2\tilde{x})} - 1) \tag{4.12}$$

while, according to (3.5) and (4.6), for $\tilde{x} = \kappa_2 x$

$$U_2(\tilde{x}) = \frac{4\pi\beta}{\kappa_2^2} \sum_{\alpha} e_\alpha^2 z_\alpha [e^{-(1/2)\,\beta e_\alpha^2 (\phi_1 - v_B)(\mathbf{r};\,\mathbf{r})} - e^{\varepsilon_\alpha}] \tag{4.13}$$

When x goes to ∞, ϕ_1 tends to the bulk value ϕ_{1B} which is the solution of

$$[\Delta_{\mathbf{r}} - \kappa_1^2]\, \phi_{1B}(\mathbf{r}, \mathbf{r}') = -4\pi\delta(\mathbf{r} - \mathbf{r}') \tag{4.14}$$

for all $\mathbf{r}$'s. As rederived below,

$$\phi_{1B}(\mathbf{r}, \mathbf{r}') = \kappa_1 \tilde{\phi}_B(\kappa_1\, |\mathbf{r} - \mathbf{r}'|) \tag{4.15}$$

with

$$\tilde{\phi}_B(\tilde{\mathbf{r}}, \tilde{\mathbf{r}}') = \frac{e^{-|\tilde{\mathbf{r}} - \tilde{\mathbf{r}}'|}}{|\tilde{\mathbf{r}} - \tilde{\mathbf{r}}'|} \tag{4.16}$$

As a consequence,

$$(\phi_{1B} - v_B)(\mathbf{r};\, \mathbf{r}) = -\kappa_1 \tag{4.17}$$

and the definitions (4.12) and (4.13) ensure that

$$\lim_{\tilde{x} \to +\infty} U_j(\tilde{x}) = 0 \tag{4.18}$$

The boundary conditions for $\tilde{\phi}_j(\tilde{x}, \tilde{x}', \mathbf{q})$ along the x-axis are the same as for $\phi_j(x, x', \mathbf{y} - \mathbf{y}')$ (see (4.5)). Moreover, since $\kappa_2 \equiv \kappa_2(\kappa_1, \varepsilon)$ a mere scaling analysis of (4.7) shows that

$$\phi_j(\mathbf{r}, \mathbf{r}';\, \kappa_j,\, \beta e^2,\, b,\, \Delta_{el}) = \kappa_j \tilde{\phi}_j(\kappa_j \mathbf{r},\, \kappa_j \mathbf{r}';\, \varepsilon,\, \kappa_j b,\, \Delta_{el}) \tag{4.19}$$

where e^2 ($\varepsilon \equiv (1/2)\,\kappa_1 \beta e^2$) is the generic notation for the e_α^2's (ε_α's).

4.3. General Solutions

In the following only the value of $\phi_j(x, x';\, \mathbf{y} - \mathbf{y}')$ for $x' > b$ will be involved and (4.7b) becomes an homogeneous equation as well as (4.7c). The simple general solutions of the latter equations that satisfy boundary conditions take the form

$$\tilde{\phi}_j(\tilde{x}, \tilde{x}', \mathbf{q};\, \tilde{b}) = \begin{cases} B_j(\tilde{x}';\, q;\, \tilde{b})(1 - \Delta_{el})\, e^{q\tilde{x}} & \text{if} \quad x < 0 \\ B_j(\tilde{x}';\, q;\, \tilde{b})[e^{q\tilde{x}} + \Delta_{el} e^{-q\tilde{x}}] & \text{if} \quad 0 < x < b \end{cases} \tag{4.20}$$

where $q \equiv |\mathbf{q}|$. The general solution of (4.7a) is the sum of a particular solution $\tilde{\phi}_j^*(\tilde{x}, \tilde{x}', \mathbf{q})$ and the general solution h_j of the corresponding homogeneous equation

$$\frac{d^2 h_j}{d\tilde{x}^2}(\tilde{x}; \mathbf{q}) + [E_q - U_j(\tilde{x})]\, h_j(\tilde{x}; \mathbf{q}) = 0 \tag{4.21}$$

with $E_q \equiv -(1+\mathbf{q}^2)$. We look for a solution h_j^+ (h_j^-) which vanishes (blows up) at large positive x,

$$\lim_{x \to +\infty} h_j^+(\tilde{x}; \mathbf{q}) = 0 \tag{4.22}$$

while $\lim_{x \to +\infty} h_j^-(\tilde{x}; \mathbf{q}) = +\infty$.

Since the $U_j(\tilde{x})$'s vanish when $\tilde{x}$ goes to $+\infty$, then, for any given positive number $\eta > 0$ there exists some $x_{q,\eta}$ such that for all $x > x_{q,\eta}$: $E_q - U_j(\tilde{x}) \leqslant -|E_q| + \eta$. As a consequence (see ref. 12) there exists one particular solution $h_j^{+*}(\tilde{x}; \mathbf{q})$ (with a particular multiplicative constant) which tends to zero when x goes to $+\infty$ at least as fast as $\exp[-\tilde{x}\sqrt{|E_q| - \eta}]$,

$$\forall \tilde{x} \geqslant \tilde{x}_{q,\eta} \qquad |h_j^{+*}(\tilde{x}; \mathbf{q})| \leqslant \exp[-\tilde{x}\sqrt{|E_q| - \eta}] \tag{4.23}$$

whereas all other solutions grow to infinity at least as fast as $\exp[\tilde{x}\sqrt{|E_q| - \eta}]$. Let call $h_j^{-*}(\tilde{x}; \mathbf{q})$ such a particular solution which diverges when $\tilde{x}$ goes to $+\infty$. Henceforth (see, for instance, ref. 14) a particular solution of (4.7a) for $x > 0$ is just

$$\tilde{\phi}_j^*(\tilde{x}, \tilde{x}', \mathbf{q}) \equiv -\frac{4\pi}{W_{j,q}}\, h_j^{-*}(\inf(\tilde{x}, \tilde{x}'); \mathbf{q})\, h_j^{+*}(\sup(\tilde{x}, \tilde{x}'); \mathbf{q}) \tag{4.24}$$

where the Wronskien $W_{j,q} \equiv h_j^{-*}(\tilde{x})(dh_j^{+*}(\tilde{x})/d\tilde{x}) - h_j^{+*}(\tilde{x})(dh_j^{-*}(\tilde{x})/d\tilde{x})$ is independent from $\tilde{x}$ because $d^2/d\tilde{x}^2 + [E_q - U_j(\tilde{x})]$ is a self-adjoint operator.

Finally, a generic solution of (4.7a) which vanishes when x goes to $+\infty$ takes the form

$$\tilde{\phi}_j(\tilde{x}, \tilde{x}', \mathbf{q}; \tilde{b}_j) = \tilde{\phi}_j^*(\tilde{x}, \tilde{x}', \mathbf{q}) + A(\tilde{x}'; \mathbf{q}, \tilde{b}_j)\, h_j^{+*}(\tilde{x}; \mathbf{q}) \qquad \text{for} \quad b < x \tag{4.25}$$

with $\tilde{b}_j \equiv \kappa_j b$. Moreover the symmetry property (4.3) implies that the solution of (4.7a) with adequate boundary conditions at $+\infty$ may be written as

$$\tilde{\phi}_j(\tilde{x}, \tilde{x}', \mathbf{q}; \tilde{b}_j) = \tilde{\phi}_j^*(\tilde{x}, \tilde{x}', \mathbf{q}) + Z(\mathbf{q}, \tilde{b}_j)\, h_j^{+*}(\tilde{x}; \mathbf{q})\, h_j^{+*}(\tilde{x}'; \mathbf{q}) \tag{4.26}$$

for $b < x$ and $b < x'$. The coefficient $Z(\mathbf{q}, \tilde{b}_j)$ is determined by the continuity relations at $\tilde{x} = \tilde{b}_j$ and $\tilde{x} = 0$ with the solutions (4.20) for $0 < x < b$ and $x < 0$.

4.4. Exact Solutions for ϕ_1 in Two Special Cases

An exact analytic expression—derived from the general method in Section 4.3—exists for the screened potential ϕ_1 in two cases. The first one corresponds to $\Delta_{el} = 0$ so that the wall has no electrostatic response for any strength ε of the Coulomb coupling inside the fluid. The second situation is the strict limit $\varepsilon = 0$ for $\Delta_{el} \neq 0$. Indeed, in both situations $U_1 = 0$ and when $x' > b$ $\tilde{\phi}_1$ is the solution $\tilde{\phi}^{(0)}(\tilde{x}, \tilde{x}', \mathbf{q}; \tilde{b}, \Delta_{el})$ of

$$\left[\frac{\partial^2}{\partial \tilde{x}^2} - (1+\mathbf{q}^2)\right] \tilde{\phi}^{(0)}(\tilde{x}, \tilde{x}', \mathbf{q}; \tilde{b}, \Delta_{el}) = -4\pi\delta(\tilde{x} - \tilde{x}') \quad \text{if} \quad b < x \tag{4.27a}$$

$$\left[\frac{\partial^2}{\partial \tilde{x}^2} - \mathbf{q}^2\right] \tilde{\phi}^{(0)}(\tilde{x}, \tilde{x}', \mathbf{q}; \tilde{b}, \Delta_{el}) = 0 \quad \text{if} \quad x < b \tag{4.27b}$$

In the following we use the notation $\tilde{b}$ for $\kappa_1 b$ and introduce $\tilde{b}_j$ only when we consider both $\kappa_1 b$ and $\kappa_2 b$.

When $\Delta_{el} = 0$, for any coupling constant ε

$$\tilde{\phi}_1(\tilde{x}, \tilde{x}', \mathbf{q}; \varepsilon, \tilde{b}, \Delta_{el} = 0) = \tilde{\phi}^{(0)}(\tilde{x}, \tilde{x}', \mathbf{q}; \tilde{b}, \Delta_{el} = 0) \tag{4.28}$$

and $\tilde{\phi}_1$ has no special property at $x = 0$. (According to (4.5), $\tilde{\phi}_1$ and $\partial\tilde{\phi}_1/\partial\tilde{x}$ are continuous at the crossing of the wall.) In fact, up to a translation of its argument x equal to b, $\tilde{\phi}_1$ is defined as the mean-field potential ϕ in the linearized Poisson–Boltzmann approximation in the case of a multicomponent plasma in the vicinity of a plain hard wall ($\Delta_{el} = 0$) located at $x = 0$. Such a wall exerts only a geometric constraint without any electrostatic attraction: there is no need for introducing the hard-core repulsion V_{SR} (2.5) involved in our generic model, so that b could be set to zero in this particular case. (We recall that at leading order in ε, the correlation (or Ursell) function of charges with a hard-core diameter σ is just equal to $-\beta e_\alpha e_{\alpha'} \phi(x, x'; \mathbf{y} - \mathbf{y}'; \Delta_{el} = 0)$[4] and does not involve σ.) As recalled in (4.26) ϕ_1 may be written as the sum

$$\tilde{\phi}^{(0)}(x, x', \kappa_1\mathbf{q}; \tilde{b}, \Delta_{el} = 0) = \tilde{\phi}_B(\kappa_1 |x - x'|, \mathbf{q}) + \tilde{h}^+_{HW}(\tilde{x} + \tilde{x}' - 2\tilde{b}; \kappa_1\mathbf{q}) \tag{4.29}$$

(see refs. 8 and 13) where $\tilde{\phi}_B$ is a particular solution of (4.27) which is chosen to be its bulk value,

$$\tilde{\phi}_B(|\tilde{x}-\tilde{x}'|, \mathbf{q}) = \frac{2\pi}{\sqrt{1+q^2}} e^{-|\tilde{x}-\tilde{x}'|\sqrt{1+q^2}} \tag{4.30}$$

and $\tilde{h}^+_{HW}$ is a solution of the associated homogeneous equation which vanishes when x goes to $+\infty$ and whose coefficient is entirely determined by the boundary conditions at the interface,

$$\tilde{h}^+_{HW}(\tilde{x}+\tilde{x}'-2\tilde{b}; \mathbf{q}) = \frac{2\pi}{\sqrt{1+q^2}} \frac{\sqrt{1+q^2}-|\mathbf{q}|}{\sqrt{1+q^2}+|\mathbf{q}|} e^{-(\tilde{x}+\tilde{x}'-2\tilde{b})\sqrt{1+q^2}} \tag{4.31}$$

However $\phi_2(\Delta_{el}=0)$ cannot be calculated explicitly, because $U_2(\tilde{x}) \neq 0$ according to (4.13) and (4.29).

When $\Delta_{el} \neq 0$, the electrostatic response of the wall disappears in the limit $\varepsilon = 0$ for $\tilde{b}$ fixed,

$$\lim_{\varepsilon \to 0} \tilde{\phi}_1(\tilde{x}, \tilde{x}', \mathbf{q}; \varepsilon, \tilde{b}, \Delta_{el}) = \tilde{\phi}^{(0)}(\tilde{x}, \tilde{x}', \mathbf{q}; \tilde{b}, \Delta_{el}) \tag{4.32}$$

where

$$\tilde{\phi}^{(0)}(\tilde{x}, \tilde{x}', \mathbf{q}; \tilde{b}, \Delta_{el}) = \tilde{\phi}_B(|\tilde{x}-\tilde{x}'|, \mathbf{q}) + Z(\mathbf{q}; \tilde{b}, \Delta_{el})\, \tilde{h}^+_{HW}(\tilde{x}+\tilde{x}'-2\tilde{b}; \mathbf{q}) \tag{4.33}$$

Z is a renormalization factor arising from the continuity conditions at $x = b$ when $\Delta_{el} \neq 0$,

$$Z(\mathbf{q}; \tilde{b}, \Delta_{el}) \equiv \frac{1-\Delta_{el} e^{-2q\tilde{b}}[\sqrt{1+q^2}+|\mathbf{q}|]^2}{1-\Delta_{el} e^{-2q\tilde{b}}[\sqrt{1+q^2}-|\mathbf{q}|]^2} \tag{4.34}$$

4.5. General Equivalent Integral Equations

According to Section 4.3 the determination of a screened potential ϕ is equivalent to solving the homogeneous equation (4.21). The asymptotic equation at large distances associated with (4.21) has two exact linearly independent solutions $A_\pm \exp[\mp\tilde{x}\sqrt{1+q^2}]$ which either vanishes or diverges when $\tilde{x}$ tends to $+\infty$. Thus, in the following $h_j^{\pm *}$ will be looked for under the form

$$h_j^{\pm *}(\tilde{x}; q, \tilde{b}) = e^{\mp\tilde{x}\sqrt{1+q^2}}[1 + H_j^{\pm *}(\tilde{x}; \sqrt{1+q^2}, \tilde{b})] \tag{4.35}$$

$h_j^{\pm *}$ is defined up to a multiplicative constant. For convenience sake, we choose the particular solution such that $h_j^{\pm *}(\tilde{b}; q, \tilde{b}) = \exp(\mp \tilde{b}\sqrt{1+q^2})$.

When $U_j(\tilde{x})$ vanishes at large distances at least as fast as $1/\tilde{x}$, we show in Appendix A that $H_j^{+*}(\tilde{x})$ is the only solution of the integral equation

$$H_j^{+*}(\tilde{x}) = -\mathscr{L}_{U_j}[1 + H_j^{+*}; 2\sqrt{1+q^2}, \tilde{b}](\tilde{x}) \tag{4.36}$$

where $\mathscr{L}_{U_j}$ is a linear operator operating on a function f as

$$\mathscr{L}_{U_j}[f; \gamma, \tilde{b}](\tilde{x}) \equiv \int_{\tilde{b}}^{\tilde{x}} dv\, e^{\gamma v} \int_v^{+\infty} dt\, e^{-\gamma t} U_j(t)\, f(t) \tag{4.37}$$

As it is the case for Dyson equation, the solution H_j^{+*} of (4.36), denoted by H_{U_j} in the following, can be written as the formal series

$$H_j^{+*} = H_{U_j} \equiv -\mathscr{L}_{U_j}[1] + \mathscr{L}_{U_j}[\mathscr{L}_{U_j}[1]] - \mathscr{L}_{U_j}[\mathscr{L}_{U_j}[\mathscr{L}_{U_j}[1]]] + \cdots \tag{4.38}$$

For the sake of conciseness we have omitted the dependence upon the parameters $\gamma = 2\sqrt{1+q^2}$ and $\tilde{b}$ in (4.38).

We notice that, similarly, the function h_j^{-*} which explodes exponentially fast when x tends to $+\infty$ and which is equal to $\exp[\tilde{b}\sqrt{1+q^2}]$ at $\tilde{x} = \tilde{b}$ corresponds to a $H_j^{-*}(u; q)$ which obeys the integral equation

$$H_j^{-*}(u; \sqrt{1+q^2}, \tilde{b}) = \int_{\tilde{b}}^{u} dv\, e^{-2v\sqrt{1+q^2}} \int_{\tilde{b}}^{v} dt\, e^{2t\sqrt{1+q^2}}\, U_j(t) \times [1 + H_j^{-*}(t; \sqrt{1+q^2}, \tilde{b})] \tag{4.39}$$

A series similar to (4.38) can be written for H_j^{-*}.

4.6. Structure of the ε-Expansions of Screened Potentials

The structure of the ε-expansions of ϕ_1 and ϕ_2 can be investigated by means of the series representation (4.38) for the intermediate object H_{U_j} combined with bounds upon U_j. First we consider $U_1(\tilde{x})$ defined in (4.12),

$$U_1(\tilde{x}) = \sum_\alpha u_{1\alpha} \left[\exp\left(\frac{\Delta_{el}\varepsilon_\alpha}{2\tilde{x}} \right) - 1 \right] \tag{4.40}$$

with $u_{1\alpha} \equiv 4\pi\beta e_\alpha^2 z_\alpha / \kappa_1^2$. As shown in Subsection B.1

$$|U_1(\tilde{x})| \leqslant \frac{|\Delta_{\rm el}|}{2}\left(\sum_\alpha u_{1\alpha}\varepsilon_\alpha\right)\frac{1}{\tilde{x}} \qquad \text{if} \quad \Delta_{\rm el} < 0 \tag{4.41}$$

$$|U_1(\tilde{x})| \leqslant \frac{\Delta_{\rm el}}{2}\left(\sum_\alpha u_{1\alpha}\varepsilon_\alpha \exp\left(\frac{\Delta_{\rm el}\varepsilon_\alpha}{2\tilde{b}}\right)\right)\frac{1}{\tilde{x}} \qquad \text{if} \quad \Delta_{\rm el} > 0 \tag{4.42}$$

The result of the ε-expansion for the solutions $h_1^{\pm *}$ of the homogeneous equation (4.21) proves to be very simple at first order in ε, as shown in Appendix B. The term of order ε in the ε-expansion of $h_1^{\pm *}$ coincides with the corresponding term in the ε-expansion of the solution of the equation (4.7a) where U_1 is replaced by its linearized value $U_1^{\rm lin}$

$$U_1^{\rm lin}(\tilde{x};\varepsilon) \equiv \left(\sum_\alpha u_{1\alpha}\varepsilon_\alpha\right)\frac{\Delta_{\rm el}}{2\tilde{x}} \tag{4.43}$$

(We stress that such a coincidence is no longer valid at higher orders in ε.) More precisely:

$$h_1^{+*}(\tilde{x};q,\tilde{b}) = e^{-\tilde{x}\sqrt{1+q^2}}\left[1+\int_{\tilde{b}}^{\tilde{x}} dv\, e^{2v\sqrt{1+q^2}}\int_v^{+\infty} dt\, e^{-2t\sqrt{1+q^2}} U_1^{\rm lin}(t;\varepsilon)\right] + \mathcal{O}_{\rm exp}(\varepsilon^2) \tag{4.44}$$

where ε is a symbolic notation for the dependence on the ε_α's. The double integral involving $U_1^{\rm lin}(t;\varepsilon)$ in (4.44) is proportional to ε, while $\mathcal{O}_{\rm exp}(\varepsilon^2)$ is equal to ε^2—possibly multiplied by some power of $\ln\varepsilon$—times a function $f(\tilde{x};\varepsilon,\tilde{b})$ which decays exponentially fast over the length-scale $\sqrt{1+q^2}$ and which is bounded for all $x > b$ by a function of $\tilde{b}$ and $\varepsilon/\tilde{b}$. The function $f(\tilde{x};\varepsilon,\tilde{b})$ may contain powers $\tilde{x}^{p(\varepsilon)}$ (with $\lim_{\varepsilon\to 0} p(\varepsilon) = 0$) times an exponential of $-\tilde{x}\sqrt{1+q^2}$, as it is the case for the exact solution of the equation (4.21) where $U_1(\tilde{x})$ is replaced by $U_1^{\rm lin}(\tilde{x})$ (see (B24)).

We point out that the correction of order ε in $h_{\rm j}^{+*}(\tilde{x};q,\tilde{b})$ is a function of $\tilde{x}$ only, whereas the higher-order corrections are functions which vary on both scales 1 and ε:

$$h_1^{+*}(\tilde{x}) = h_1^{(0)+}(\tilde{x}) + \varepsilon h_1^{(1)+}(\tilde{x}) + \varepsilon^2 h_1^{(2)+}\left(\tilde{x},\frac{\tilde{x}}{\varepsilon}\right) + \mathcal{O}(\varepsilon^3) \tag{4.45}$$

This property ensures that the zeroth order term in the ε-expansion of the derivative $\partial h_1^{+*}/\partial\tilde{x}$ depends only on the corresponding term in the

ε-expansion of h_1^{+*}, whereas the first-order term involves the derivatives of both the first and second corrections to h_1^{+*},

$$\frac{\partial h_1^{+*}}{\partial \tilde{x}} = \frac{dh_1^{(0)+}(\tilde{x})}{d\tilde{x}} + \varepsilon \left[\frac{dh_1^{(1)+}(\tilde{x})}{d\tilde{x}} + \frac{\partial h_1^{(2)+}(\tilde{x}, u)}{\partial u}\bigg|_{u=\tilde{x}/\varepsilon} \right] + \mathcal{O}(\varepsilon^2) \tag{4.46}$$

According to (4.39), results similar to (4.44) and (4.45) also hold for $h_1^{-*}(\tilde{x})$.

Finally, we turn to the ε-expansion for the screened potential ϕ_1. ϕ_1 is calculated from the $h_1^{\pm *}$'s by using the expression (4.26) valid for $x > b$ together with the continuity relations (4.5) involving the solutions (4.20) in the region $x < b$. As a consequence of (4.46), at leading order in ε, the continuity relation (4.5) for the derivative $\partial\phi_1/\partial\tilde{x}$ involves only the $h_1^{(0)\pm}$'s and their derivatives $dh_1^{(0)\pm}/d\tilde{x}$. Therefore, the leading term $\tilde{\phi}_1^{(0)}$ in the ε-expansion of ϕ_1 is entirely determined by the functions $h_1^{(0)+}$ and $h_1^{(0)-}$ (and not by functions which appear at higher orders in the ε-expansions of the $h_1^{*\pm}$'s) and it coincides with $\tilde{\phi}^{(0)}$ given in (4.33),

$$\phi_1(\mathbf{r}, \mathbf{r}') = \kappa_1 \tilde{\phi}^{(0)}(\kappa_1 \mathbf{r}, \kappa_1 \mathbf{r}'; \kappa_1 b, \Delta_{\text{el}}) + \kappa_1 \mathcal{O}_{\text{exp}}(\varepsilon) \tag{4.47}$$

where $\mathcal{O}_{\text{exp}}(\varepsilon)$ has the same meaning as in (4.44). As a consequence of (4.47)

$$-\tfrac{1}{2}\beta e_\alpha^2 [\phi_1 - \phi_{\text{B}}](\mathbf{r}, \mathbf{r}) = \varepsilon_\alpha F(\tilde{x}; \varepsilon, \tilde{b}) \tag{4.48}$$

where $F(\tilde{x}; \varepsilon, \tilde{b})$ is a continuous function of $\tilde{x}$ in the interval $b \leqslant \tilde{x} < \infty$ which decays exponentially fast (with possible multiplicative powers $x^{p(\varepsilon)}$) over a typical length 1 when $\tilde{x}$ goes to $+\infty$. $F(\tilde{x}; \varepsilon, \tilde{b})$ is integrable when $\tilde{x}$ goes to $+\infty$ even when ε vanishes, and may be bounded as follows,

$$|F(\tilde{x}; \varepsilon, \tilde{b})| \leqslant M_F(\varepsilon/\tilde{b})\, g(\tilde{x}) \qquad \forall \tilde{x} \geqslant \tilde{b} \tag{4.49}$$

where $g(\tilde{x})$ is continuous and integrable in the interval $[\tilde{b}, +\infty[$.

From the previous result, we get the structure of $U_2(\tilde{x})$ given in (4.13). For $\tilde{x} = \kappa_2 x$

$$U_2(\tilde{x}) = \sum_\alpha u_{2\alpha} [e^{\varepsilon_\alpha F(\tilde{x}(\kappa_1/\kappa_2); \varepsilon, \tilde{b})} - 1] \tag{4.50}$$

with $u_{2\alpha} \equiv 4\pi\beta e_\alpha^2 z_\alpha \exp(\varepsilon_\alpha)/\kappa_2^2$. We show in Appendix B that, as it is the case for U_1, the first terms in the ε-expansion of h_2^{+*} are given by (4.44) where $U_1^{\text{lin}}(\tilde{x}; \varepsilon)$ is replaced by

$$U_2^{\text{lin}}(\tilde{x}; \varepsilon, \tilde{b}) = \sum_\alpha u_{2\alpha} \varepsilon_\alpha F(\tilde{x}\kappa_1/\kappa_2; \varepsilon, \tilde{b}) \tag{4.51}$$

The double integral involving $U_2^{\text{lin}}(t; \varepsilon, \tilde{b})$ in (4.44) is not merely proportional to ε. According to definitions (4.8) and (4.9)

$$\kappa_2 = \kappa_1[1 + \mathcal{O}(\varepsilon)] \tag{4.52}$$

and the properties of the double integral at stake imply that the first two terms in the ε-expansion of h_2^{+*} are given by (4.44) where U_2^{lin} is replaced by

$$\left(\sum_{\alpha} u_{2\alpha}\varepsilon_{\alpha}\right) F(\tilde{x}; \varepsilon = 0, \tilde{b}) \tag{4.53}$$

Subsequently, all properties derived from (4.44) also hold for h_2^{+*}.

Eventually, the main result of the previous perturbative analysis is that, at leading order in ε, ϕ_1 and ϕ_2 coincide with the same function $\phi^{(0)}$ apart from a scaling dependence upon either κ_1 or κ_2

$$\phi_j(x, x', \kappa_j\mathbf{q}; \varepsilon, \kappa_j b, \Delta_{\text{el}}) = \frac{1}{\kappa_j}\tilde{\phi}^{(0)}(\kappa_j x, \kappa_j x', \mathbf{q}; \kappa_j b, \Delta_{\text{el}}) + \frac{1}{\kappa_j}\mathcal{O}_{\exp}(\varepsilon) \tag{4.54}$$

In (4.54) $\mathcal{O}_{\exp}(\varepsilon)$ denotes a function of the variable x which satisfies two properties. First it decays exponentially fast over the scale κ_j in the sense that it falls off as $\exp(-\kappa_j x\sqrt{1+q^2})$ times a function which may increase as $x^{p(\varepsilon)}$ with $\lim_{\varepsilon\to 0} p(\varepsilon) = 0$. Second, $\mathcal{O}_{\exp}(\varepsilon)$ remains bounded by ε—possibly multiplied by some power of $\ln\varepsilon$—times a function of $\varepsilon/(\kappa_1 b) \propto \beta e^2/b$ for all $x > b$, even if $\mathcal{O}_{\exp}(\varepsilon)$ may drastically vary over the scale $\varepsilon\kappa_j \sim \beta e^2 \ll \kappa_j$.

As shown in next section, because of the neutrality constraint (2.13), the explicit value of the correction of order ε in ϕ_2 happens not to appear in the first correction to the density profile. (Only some properties of it must be known in order to settle that it really does not contribute to the density profile at order ε). The latter result may be viewed as a consequence of the following property, already used in ref. 4. According to the first equation of the BGY hierarchy, the first-order correction induced by Coulomb interactions in the density profile is determined only by the potential drop $\Phi(x)$ and the Ursell function at leading order; besides the latter one is nothing but the screened potential ϕ_2 in the limit $\varepsilon = 0$. We recall that $\lim_{\varepsilon\to 0}\phi_2$ is drastically different from the bare long-ranged Coulomb potential v_{w}, which would be a too crude approximation for the Ursell function: though $\lim_{\varepsilon\to 0}\phi_2$ has the same amplitude βe^2 as v_{w}, it is a short-ranged function with a characteristic scale $\kappa \propto \varepsilon/(\beta e^2)$.

5. SCALING ANALYSIS IN THE WEAK-COUPLING LIMIT

In the weak-coupling regime of interest, the particle density $\rho_\alpha(x)$ at leading order in ε is equal to its value $\rho_\alpha^{\mathrm{id}}(x)$ in an ideal gas submitted to the external potential corresponding to the self-energy $-\Delta_{\mathrm{el}} e_\alpha^2/4x$ of a charge in the presence of a wall with an electrostatic response,

$$\rho_\alpha^{\mathrm{id}}(x) = z_\alpha \exp(\Delta_{\mathrm{el}} \beta e_\alpha^2/4x) \tag{5.1}$$

According to (1.8) and (4.8), the small dimensionless coupling parameter inside the Coulomb fluid may be chosen as

$$\varepsilon_\alpha \equiv \tfrac{1}{2}\kappa_1 \beta e_\alpha^2 \ll 1 \tag{5.2}$$

while the coupling constant with the dielectric wall

$$\frac{\Delta_{\mathrm{el}} \beta e_\alpha^2}{4b} \tag{5.3}$$

can take any finite given value.

5.1. Screened Fugacities

In the weak-coupling regime, a simple scaling analysis may be performed in the bulk as in the inhomogeneous situation near the wall. As a consequence of (4.54) $(1/2)\,\beta e_\alpha^2(\phi_1 - v_{\mathrm{B}})(\mathbf{r}, \mathbf{r})$ scales as ε_α at leading order and takes the generic form

$$-\tfrac{1}{2}\beta e_\alpha^2(\phi_1 - v_{\mathrm{B}})(\mathbf{r}; \mathbf{r}) = \varepsilon_\alpha\{1 - L(\kappa_1(x-b); \kappa_1 b, \Delta_{\mathrm{el}})\} + \mathcal{O}_{\exp}(\varepsilon^2) \tag{5.4}$$

where the term of leading order is entirely determined by $\kappa_1 \tilde{\phi}^{(0)}(\kappa_1 \mathbf{r}, \kappa_1 \mathbf{r}; \kappa_1 b, \Delta_{\mathrm{el}})$,

$$L(\tilde{x} - \tilde{b}; \tilde{b}, \Delta_{\mathrm{el}}) = \int \frac{d^2\mathbf{q}}{(2\pi)^2} [\tilde{\phi}^{(0)}(\tilde{x}, \tilde{x}, \mathbf{q}; \tilde{b}, \Delta_{\mathrm{el}}) - \tilde{\phi}_{\mathrm{B}}(\tilde{x}, \tilde{x}, \mathbf{q})] \tag{5.5}$$

$L(\tilde{x} - \tilde{b}; \tilde{b}, \Delta_{\mathrm{el}})$ has been studied in Section 3.2 of Paper I. It can be decomposed into

$$L(\tilde{x} - \tilde{b}; \tilde{b}, \Delta_{\mathrm{el}}) = -\Delta_{\mathrm{el}} \frac{e^{-2\tilde{x}}}{2\tilde{x}} + \bar{L}(\tilde{x}; \tilde{b}, \Delta_{\mathrm{el}}) \tag{5.6}$$

where $\bar{L}(\tilde{x}-\tilde{b};\tilde{b},\Delta_{\rm el})$ remains finite even when $\tilde{x}=\tilde{b}=0$. Thus, according to (3.5), (5.4) and (5.6), $\bar{z}_\alpha^{[1]}$ proves to read

$$\bar{z}_\alpha^{[1]}(x)=z_\alpha e^{\varepsilon_\alpha}\,\theta(x-b)\exp\left[\Delta_{\rm el}\frac{\beta e_\alpha^2}{4x}e^{-2\kappa_1 x}\right]$$
$$\times\{1-\varepsilon_\alpha\bar{L}(\kappa_1 x;\kappa_1 b,\Delta_{\rm el})+\mathcal{O}_{\exp}(\varepsilon^2)\} \tag{5.7}$$

The expression (3.7) of $\bar{z}_\alpha^{[2]}$ differs from the expression (3.5) of $\bar{z}_\alpha^{[1]}$ only by the replacement of ϕ_1 by ϕ_2. At leading order in ε, apart from the change of κ_1 into κ_2, ϕ_2 coincides with ϕ_1 (see (4.54)). Thus $\bar{z}_\alpha^{[2]}$ is given by (5.7) where κ_1 is replaced by κ_2 and ε_α is multiplied by κ_2/κ_1. However, according to (4.9),

$$\frac{\kappa_2}{\kappa_1}\varepsilon_\alpha=\varepsilon_\alpha[1+\mathcal{O}(\varepsilon)] \tag{5.8}$$

so that

$$\bar{z}_\alpha^{[2]}(x)=\theta(x-b)\,z_\alpha\exp\left[\Delta_{\rm el}\frac{\beta e_\alpha^2}{4x}e^{-2\kappa_2 x}\right]$$
$$\times\{1+\varepsilon_\alpha[1-\bar{L}(\kappa_2 x;\kappa_2 b,\Delta_{\rm el})]+\mathcal{O}_{\exp}(\varepsilon^2)\} \tag{5.9}$$

We remind the reader that $\mathcal{O}_{\exp}(\varepsilon^2)$ denotes a function which tends exponentially fast to a constant of order ε^2—possibly multiplied by some power of $\ln\varepsilon$—when x goes to $+\infty$.

5.2. Diagrams Contributing at Leading Order in ε

First, we notice that even in the case where L is not bounded at the origin—as it is the case when $\epsilon_{\rm w}>1$—an ε-expansion can be performed for integrals of the form $\int d\mathbf{r}'\,\bar{z}_\gamma^{[2]}(x')\,f(\mathbf{r},\mathbf{r}')$. For that purpose, we introduce

$$w_0(\tilde{x};\varepsilon_\alpha,\Delta_{\rm el})\equiv\exp\left[\Delta_{\rm el}\frac{\varepsilon_\alpha}{2\tilde{x}}e^{-2\tilde{x}}\right]-1 \tag{5.10}$$

and we use the following formulas. Let us consider a dimensionless function f of the variable x which involves two length scales l_1 and l_2. f may be written as $f(x/l_2;l_1/l_2)$. We set $\varepsilon\equiv l_1/l_2$. When $b>l_2$, for all $x>b$ x/l_2 remains finite when ε vanishes and

$$\operatorname*{Exp}_{\varepsilon\to 0}\left[\int_b^{+\infty}dx\,f(x/l_2;\varepsilon)\right]=l_2\int_{b/l_2}^{+\infty}d\tilde{x}_2\operatorname*{Exp}_{\varepsilon\to 0}[f(\tilde{x}_2;\varepsilon)] \tag{5.11}$$

When $b \ll l_2$, we use the identity

$$\operatorname*{Exp}_{l_1 \ll l_2} \int_b^\infty dx \cdots = \operatorname*{Exp}_{l_1 \ll l \ll l_2} \left[\int_b^l dx \cdots + \int_l^\infty dx \cdots \right] \tag{5.12}$$

When l/l_2 vanishes, x/l_2 goes to zero for all $x < l$ but remains finite for any $x > l$. Thus a basic formula for ε-expansions when $b \ll l_2$ reads

$$\operatorname*{Exp}_{\varepsilon \to 0} \left[\int_b^{+\infty} dx\, f(x/l_2; \varepsilon) \right] = \operatorname*{Exp}_{l/l_1 \to +\infty} \operatorname*{Exp}_{l/l_2 \to 0} \left\{ l_1 \int_{b/l_1}^{l/l_1} d\tilde{x}_1 \operatorname*{Exp}_{\varepsilon \to 0} [f(\varepsilon \tilde{x}_1; \varepsilon)] + l_2 \int_{l/l_2}^{+\infty} d\tilde{x}_2 \operatorname*{Exp}_{\varepsilon \to 0} [f(\tilde{x}_2; \varepsilon)] \right\} \tag{5.13}$$

We notice that only the sum of the two integrals in (5.13) is independent from l, whereas the first (second) integral may diverge when l/l_1 becomes infinite (when l/l_2 vanishes). Whatever the value of b may be, (5.11) and (5.13) imply that $\kappa_D \int d\mathbf{r}'\, w_0(x'; \varepsilon_\alpha, \Delta_{\text{el}})\, f(\mathbf{r}, \mathbf{r}')$ is at least of order $\varepsilon \ln \varepsilon$ (see also Subsection 3.3 of Paper I).

The simplest diagrams contributing to $\rho_\alpha(x)$ are written in (3.11). The potential involved in F^{cc} is ϕ_2. First, the scaling property of ϕ_2 at leading order in ε, namely

$$\phi_2^{(0)}(\mathbf{r}, \mathbf{r}'; \kappa_2) = \kappa_2 \tilde{\phi}^{(0)}(\kappa_2 \mathbf{r}, \kappa_2 \mathbf{r}'), \tag{5.14}$$

implies that, according to (3.8), (4.9), (5.2) and (5.9),

$$\int d\mathbf{r}'\, \bar{z}_\gamma^{[2]}(x')\, F^{\text{cc}}(\mathbf{r}; \mathbf{r}') = \mathcal{O}(\varepsilon^0) \tag{5.15}$$

Moreover, this leading correction depends on the species only through a coefficient z_γ. Subsequently, according to the neutrality constraint (2.13), after summation over species, the diagram with one bond F^{cc} contributes only at next order in ε,

$$\sum_\gamma \int d\mathbf{r}'\, \bar{z}_\gamma^{[2]}(x')\, F^{\text{cc}}(\mathbf{r}; \mathbf{r}') = \mathcal{O}(\varepsilon) \tag{5.16}$$

In the same way, the scaling argument shows that

$$\int d\mathbf{r}'\, \bar{z}_\alpha^{[2]}(x') [F^{\text{cc}}(\mathbf{r}; \mathbf{r}')]^2 = \mathcal{O}(\varepsilon) \tag{5.17}$$

An ε-expansion can be performed for the contribution from $[F^{cc}]^2$ to the density representation (3.11). Since $\bar{L}(\kappa_j x)$ decays exponentially fast, comparison of (5.7) and (5.9) implies with (5.8) that

$$\bar{z}_\alpha^{[2]}(x) = \bar{z}_\alpha^{[1]}(x) \times \exp\left[\Delta_{el} \frac{\beta e_\alpha^2}{2x} (e^{-2\kappa_2 x} - e^{-2\kappa_1 x}) \right] + \mathcal{O}(z_\alpha \varepsilon^2) \tag{5.18}$$

and a straightforward calculation leads to the result

$$\int d\mathbf{r}' \, [\bar{z}_\alpha^{[2]}(x') - \bar{z}_\alpha^{[1]}(x')][F^{cc}(\mathbf{r}; \mathbf{r}')]^2 = \mathcal{O}(\varepsilon^2) \tag{5.19}$$

The basic formulas (5.11) and (5.13) with $l_1 = \beta e_\alpha e_\gamma$ and $l_2 = \kappa_2^{-1}$ allow one to show that

$$\int d\mathbf{r}' \, \bar{z}_\alpha^{[2]}(x') \, F_{RT}(\mathbf{r}; \mathbf{r}') = \mathcal{O}(\varepsilon^2) \tag{5.20}$$

Indeed, according to (3.10) and (5.14), the scaling change $\mathbf{r} = \tilde{\mathbf{r}}/\kappa_2$ shows that

$$\begin{aligned} \tilde{F}_{RT}(\tilde{\mathbf{r}}; \tilde{\mathbf{r}}'; \varepsilon_{\alpha\gamma}) = \theta(\|\tilde{\mathbf{r}} - \tilde{\mathbf{r}}'\| - \kappa_2 \sigma) \, e^{-\varepsilon_{\alpha\gamma} \tilde{\phi}_2(\tilde{\mathbf{r}}; \tilde{\mathbf{r}}')} - 1 \\ + \varepsilon_{\alpha\gamma} \tilde{\phi}_2(\tilde{\mathbf{r}}; \tilde{\mathbf{r}}') - \tfrac{1}{2} \varepsilon_{\alpha\gamma}^2 (\tilde{\phi}_2(\tilde{\mathbf{r}}; \tilde{\mathbf{r}}'))^2 \end{aligned} \tag{5.21}$$

with $\varepsilon_{\alpha\gamma} \equiv \kappa_2 \beta e_\alpha e_\gamma$. Since $\bar{z}_\alpha^{[2]}$ scales as $z_\alpha = \rho_{\alpha B}^{id} \propto 1/a^3$ (where $\rho_{\alpha B}^{id}$ is the bulk density of an ideal gas with the same fugacities) and

$$\operatorname*{Exp}_{\varepsilon \to 0} \tilde{F}_{RT}(\tilde{\mathbf{r}}; \tilde{\mathbf{r}}'; \varepsilon_{\alpha\gamma}) = \mathcal{O}(\varepsilon_{\alpha\gamma}^3), \tag{5.22}$$

$\int d\mathbf{r}' \, \bar{z}_\alpha^{[2]}(x') \, F_{RT}(\mathbf{r}; \mathbf{r}')$ is of order $\kappa_2^{-3} a^{-3} \varepsilon_{\alpha\gamma}^3 = \mathcal{O}(\varepsilon_{\alpha\gamma}^2)$. (See definitions (1.6) and (1.8).) We notice that the same result is obtained by using the scaling change $\mathbf{r} = \beta e_\alpha e_\gamma \mathbf{u}$ and the property that $\lim_{\varepsilon \to 0} F_{RT}(\varepsilon \mathbf{u}, \varepsilon \mathbf{u}'; \varepsilon_{\alpha\gamma})$ is an integrable function of $\mathbf{u}$ independent from ε so that (5.13) implies that $\int d\mathbf{r}' \, \bar{z}_\alpha^{[2]}(x') \, F_{RT}(\mathbf{r}; \mathbf{r}')$ is of order $(\beta e_\alpha e_{\alpha'})^3 a^{-3} = \mathcal{O}(\Gamma^3) = \mathcal{O}(\varepsilon^2)$. In fact, the lengths b and σ may also generate contributions of order $\varepsilon^2 \exp[\Delta_{el} \beta e_\alpha^2 / 4b]$ or $\varepsilon^2 \exp[\beta e_\alpha^2 / \sigma]$, where b and σ are supposed to be finite.

A scaling analysis analogous to that performed in ref. 3 shows that more complicated diagrams contribute at least at the order ε^2 in the exponential of the diagrammatic representation (3.11). Eventually, in order to calculate $\rho_\alpha(x)$ up to order ε, in (3.11) we only have to consider the contribution from the diagram with one bond F^{cc} up to order ε.

5.3. ε-Expansions of the Contribution from the F^{cc} Diagram

In (3.11) the contribution from F^{cc} up to order ε is derived from (3.8), where ϕ_2 is replaced by its leading value $\phi_2^{(0)}$, and (5.9). It is equal to the first order term in the ε-expansion of

$$-\frac{\beta e_\alpha}{\kappa_2^2}\int_{\tilde b}^{+\infty} d\tilde x' \sum_\gamma z_\gamma e_\gamma [1+w_0(\tilde x';\varepsilon_\gamma,\Delta_{el})]\{1+\varepsilon_\gamma[1-\bar L(\tilde x';\tilde b,\Delta_{el})]+\mathcal{O}_{exp}(\varepsilon^2)\}$$
$$\times\{\tilde\phi^{(0)}(\tilde x,\tilde x',\mathbf{q}=\mathbf{0};\tilde b)+\tilde\phi^{(1)}(\tilde x,\tilde x',\mathbf{q}=\mathbf{0};\tilde b,\Delta_{el})+\mathcal{O}_{exp}(\varepsilon^2)\} \tag{5.23}$$

where $\tilde b=\kappa_2 b$ and $w_0(\tilde x;\varepsilon_\alpha,\Delta_{el})$ is defined in (5.10). According to the neutrality constraint (2.13) and since the function $\tilde\phi$ does not depend on the species γ, while the integral of $f(\tilde x)$ times $w_0(\tilde x;\varepsilon_\alpha,\Delta_{el})$ gives a contribution of order larger than $\int d\tilde x\, f(\tilde x)$, the contribution (5.23) involves only the leading term in the potential ϕ_2; it is reduced to

$$-\frac{\beta e_\alpha}{\kappa_2^2}\int_{\tilde b}^{+\infty} d\tilde x' \sum_\gamma z_\gamma e_\gamma\{w_0(\tilde x';\varepsilon_\gamma,\Delta_{el})+\varepsilon_\gamma[1-\bar L(\tilde x';\tilde b,\Delta_{el})]\}$$
$$\times\tilde\phi^{(0)}(\tilde x,\tilde x',\mathbf{q}=\mathbf{0};\tilde b) \tag{5.24}$$

where $\tilde\phi^{(0)}(\tilde x,\tilde x',\mathbf{q}=\mathbf{0};\tilde b)=2\pi\,[e^{-|\tilde x-\tilde x'|}+e^{-(\tilde x+\tilde x'-2\tilde b)}]$.

Equation (5.24) may be rewritten as

$$\sum_\gamma\int d\mathbf{r}'\,\bar z_\gamma^{[2]}(x')\,F^{cc}(\mathbf{r};\mathbf{r}')$$
$$=-\frac{4\pi\beta e_\alpha}{\kappa_2^2}\left(\sum_\gamma z_\gamma e_\gamma\varepsilon_\gamma[1-M_\gamma(\kappa_2 x;\varepsilon_\gamma,\kappa_2 b,\Delta_{el})]\right)+\mathcal{O}_{exp}(\varepsilon^2) \tag{5.25}$$

where $M_\gamma=\bar M+[M_\gamma-\bar M]$ with

$$\bar M(\tilde x;\tilde b,\Delta_{el})=\tfrac12\int_{\tilde b}^{+\infty} du'\,[e^{-|\tilde x-u'|}+e^{-(\tilde x+u'-2\tilde b)}]\,\bar L(u';\tilde b,\Delta_{el}) \tag{5.26}$$

and $M_\gamma-\bar M$ is the ε-expansion at orders $\ln\varepsilon_\gamma$ and $(\varepsilon_\gamma)^0$ of the integral

$$-\frac12\frac{1}{\varepsilon_\gamma}\int_{\tilde b}^{+\infty} du'\,[e^{-|\tilde x-u'|}+e^{-(\tilde x+u'-2\tilde b)}]\,w_0(u';\varepsilon_\gamma,\Delta_{el}) \tag{5.27}$$

5.4. Structure of the ε-Expansion for the Density Profile

The structure of the ε-expansion for the density profile can now be investigated. According to (3.11) and the results of the previous section

$$\rho_\alpha(x) = \bar{z}_\alpha^{[2]}(x)\left[1+\sum_\gamma \int d\mathbf{r}'\, \bar{z}_\gamma^{[2]}(x')\, F^{cc}(\mathbf{r},\mathbf{r}';\alpha,\gamma)\right][1+\mathcal{O}_{exp}(\varepsilon^2)] \tag{5.28}$$

where $\bar{z}_\alpha^{[2]}(x)$ is given by (5.9) and $F^{cc}(\mathbf{r},\mathbf{r}';\alpha,\gamma)$ is replaced by $-\beta e_\alpha e_\gamma \kappa_2 \tilde{\phi}^{(0)}(\kappa_2\mathbf{r}, \kappa_2\mathbf{r}')$. By using (5.25) we get

$$\rho_\alpha(x) = \theta(x-b)\, z_\alpha \exp\left(\Delta_{el}\frac{\beta e_\alpha^2}{4x}e^{-2\kappa_2 x}\right)\left\{1+\varepsilon_\alpha[1-\bar{L}(\kappa_2 x;\kappa_2 b,\Delta_{el})]\right.$$
$$\left.-\frac{4\pi\beta e_\alpha}{\kappa_2^2}\sum_\gamma z_\gamma e_\gamma \varepsilon_\gamma[1-M_\gamma(\kappa_2 x;\varepsilon_\gamma,\kappa_2 b,\Delta_{el})]+\mathcal{O}_{exp}(\varepsilon^2)\right\} \tag{5.29}$$

By definition of the bulk density (2.11) and since $\bar{L}$ and M_γ vanish when x goes to infinity

$$\rho_\alpha^B = z_\alpha\left\{1+\varepsilon_\alpha-\frac{(\sum_\gamma z_\gamma e_\gamma \varepsilon_\gamma)\,4\pi\beta e_\alpha}{\kappa_2^2}+\mathcal{O}(\varepsilon^2)\right\} \tag{5.30}$$

The latter expression does coincide with the classical limit of the particle density in a quantum plasma where exchange effects are neglected (see Eq. (5.28) in ref. 1). Moreover, according to (1.6) and (4.9), κ_2 is equal to κ_D up to a correction of order ε

$$\kappa_2 = \kappa_D[1+\mathcal{O}(\varepsilon)] \tag{5.31}$$

Using the property $\exp[-(1+\varepsilon)u] = \exp[-u]-\varepsilon u\exp[-u]+\mathcal{O}(\varepsilon^2 u)$, comparison of (5.29) with (5.30) leads to

$$\rho_\alpha(x) = \rho_\alpha^B\theta(x-b)\exp\left(\Delta_{el}\frac{\beta e_\alpha^2}{4x}e^{-2\kappa_D x}\right)\times\left\{1-\frac{1}{2}\beta\kappa_D\left[e_\alpha^2\bar{L}(\kappa_D x;\kappa_D b,\Delta_{el})\right.\right.$$
$$\left.\left.-e_\alpha\frac{4\pi\beta}{\kappa_D^2}\sum_\gamma \rho_\gamma^B e_\gamma^3 M_\gamma(\kappa_D x;\varepsilon_\gamma,\kappa_D b,\Delta_{el})\right]+\mathcal{O}_{exp}(\varepsilon^2)\right\} \tag{5.32}$$

where $\varepsilon_\gamma = (1/2)\,\beta e_\gamma^2\kappa_D$.

The term with M_γ in (5.32) is related to the electrostatic potential drop $\Phi(x)$ created by the charge density profile. Indeed, when the relation between $\Phi(x)$ and the corresponding electrostatic field is combined with

Gauss theorem together with the symmetries of the problem, and after an integration by parts, $\Phi(x)$ proves to read

$$\Phi(x) = -4\pi \int_x^{+\infty} dx' \, (x'-x) \sum_\alpha e_\alpha \rho_\alpha(x') \tag{5.33}$$

(The value of $\Phi(x)$ when x goes to $+\infty$ is chosen to be equal to zero). When the structure (5.28) of $\rho_\alpha(x)$ is inserted into (5.33), according to (5.9) (5.11) and (5.13), the contribution to $\Phi(x)$ at leading order ε only comes from the following part in $\rho_\alpha(x)$ (with $x > b$),

$$\bar{z}_\alpha^{[2]}(x) + z_\alpha \, (-\beta e_\alpha) \, G(x) \tag{5.34}$$

where

$$G(x) = \int d\mathbf{r}' \sum_\gamma e_\gamma \bar{z}_\gamma^{[2]}(x') \, \kappa_2 \tilde{\phi}^{(0)} \, (\kappa_2 \mathbf{r}, \kappa_2 \mathbf{r}') \tag{5.35}$$

Since $\tilde{\phi}^{(0)} \, (\tilde{x}, \tilde{x}', \mathbf{q})$ obeys equation (4.27a),

$$\kappa_2^2 \, G(x) = 4\pi \sum_\gamma e_\gamma \bar{z}_\gamma^{[2]}(x) + \frac{d^2 G(x)}{dx^2} \tag{5.36}$$

when $x > b$. Moreover $\kappa_2^2 = 4\pi\beta(\sum_\alpha z_\alpha e_\alpha^2) \times [1 + \mathcal{O}(\varepsilon)]$ so that

$$\Phi(x) = \left[\int_x^{+\infty} dx'(x'-x) \frac{d^2 G(x')}{dx'^2} \right] [1 + \mathcal{O}_{\exp}(\varepsilon)] \tag{5.37}$$

According to the decay property of $\tilde{\phi}^{(0)}$, $G(x)$ tends to a constant exponentially fast when x goes to $+\infty$. Thus, after integration by parts, (5.37) leads to

$$\Phi(x) = [G(x) - \lim_{x \to +\infty} G(x)][1 + \mathcal{O}_{\exp}(\varepsilon)] \tag{5.38}$$

Since $-\beta e_\alpha G(x)$ coincides with the l.h.s. of (5.25) at leading order in ε, the explicit value of $\Phi(x)$ is given by

$$\Phi(x) = -\frac{2\pi\beta}{\kappa_D} \sum_\gamma \rho_\gamma e_\gamma^3 M_\gamma(\kappa_D x; \varepsilon_\gamma, \kappa_D b, \Delta_{\text{el}}) + \mathcal{O}_{\exp}(\varepsilon^2/\beta e) \tag{5.39}$$

The latter result ensures that the expression of the density profile derived in Paper I from a mean-field approach is exact at leading order in ε_D.

APPENDIX A

In this appendix we show that, when $U_j(\tilde{x})$ vanishes at large distances at least as fast as $1/\tilde{x}$, $H_j^{+*}(\tilde{x})$ defined in (4.35) is the only solution of the integral equation (4.36). $H_j^{+*}(x; \sqrt{1+q^2}, \tilde{b})$ obeys the nonhomogeneous differential equation

$$\frac{d^2H_j^+}{d\tilde{x}^2} - 2\sqrt{1+q^2}\frac{dH_j^+}{d\tilde{x}} - U_j(\tilde{x})\, H_j^+ = U_j(\tilde{x}) \tag{A1}$$

and satisfies the following boundary conditions

$$H_j^{+*}(\tilde{b}; \sqrt{1+q^2}, \tilde{b}) = 0 \tag{A2}$$

and

$$\lim_{\tilde{x} \to +\infty} e^{-\tilde{x}\sqrt{1+q^2}} H_j^{+*}(\tilde{x}; \sqrt{1+q^2}, \tilde{b}) = 0 \tag{A3}$$

By using the extra change of function $G_j(\tilde{x}) = \exp[-2\tilde{x}\sqrt{1+q^2}]$ $\times dH_j^+/d\tilde{x}$ the problem is reduced to a first-order differential equation which relates $dG_i/d\tilde{x}$ to H_j^+. The formal integration of the latter equation leads to the relation

$$H_j^+(\tilde{x}; \sqrt{1+q^2}, \tilde{b}) = a_0 + a_1 e^{2\tilde{x}\sqrt{1+q^2}} - \mathscr{L}_{U_j}[1 + H_j^+; 2\sqrt{1+q^2}, \tilde{b}] \tag{A4}$$

where $\mathscr{L}_{U_j}$ is the linear operator defined in (4.37).

When U_j tends to zero at least as fast as $U_0/\tilde{x}$ when $\tilde{x}$ goes to infinity (with U_0 a constant), the boundary conditions (A2) and (A3) imply that the integration constants a_0 and a_1 are in fact equal to zero in the case of H_j^{+*}. Indeed, the hypothesis about U_j means that there exists some $\tilde{x}_0$ such that

$$\forall \tilde{x} \geqslant \tilde{x}_0 \qquad |U_j(\tilde{x})| \leqslant \frac{U_0}{\tilde{x}} \tag{A5}$$

On the other hand, according to (A3), for any given real $M > 0$ there exists some $\tilde{x}_1$ such that

$$\forall \tilde{x} \geqslant \tilde{x}_1(M) \qquad e^{-\tilde{x}\sqrt{1+q^2}} |1 + H_j^{+*}(\tilde{x})| < M \tag{A6}$$

Since $\exp(\gamma v)$ is an increasing function of v, (A5) and (A6) combined with properties of integrals lead to the inequality

$$|\mathscr{L}_{U_j}[1+H_j^{+*}; 2\sqrt{1+q^2}, \tilde{b}](\tilde{x})| \leqslant \mathscr{L}_{|U_j|}[1+H_j^{+*}; 2\sqrt{1+q^2}, \tilde{b}](\tilde{x}_2) + MU_0 e^{\tilde{x}\sqrt{1+q^2}} \mathscr{L}_{1/t}[1; \sqrt{1+q^2}, \tilde{x}_2](\tilde{x}) \tag{A7}$$

with $\tilde{x}_2 = \sup(\tilde{x}_0, \tilde{x}_1)$. In (A7), the left term in the upper bound is independent from $\tilde{x}$ while the right term can be calculated explicitly. An integration by parts leads to the result

$$\mathscr{L}_{1/t}[1; \gamma, \tilde{b}](\tilde{x}) = \frac{1}{\gamma}[\ln(\gamma\tilde{x}) + B(\gamma\tilde{x}; \gamma\tilde{b})] \tag{A8}$$

where $B(\gamma\tilde{x}; \gamma\tilde{b})$ is a continuous function of $\tilde{x}$ which has a finite limit when $\tilde{x}$ goes to $+\infty$ and which tends to $-\ln\tilde{b}$ when $\tilde{x}$ approaches the value $\tilde{b}$. Indeed,

$$B(\gamma\tilde{x}; \gamma\tilde{b}) \equiv -[e^{\gamma\tilde{x}}\,\mathrm{Ei}(-\gamma\tilde{x}) - e^{\gamma\tilde{b}}\,\mathrm{Ei}(-\gamma\tilde{b})] - \ln(\gamma\tilde{b}) \tag{A9}$$

where $\mathrm{Ei}(-u)$ denotes the Exponential–Integral function defined for $u > 0$ as $\mathrm{Ei}(-u) \equiv -\int_u^{+\infty} dt \exp(-t)/t$. As a consequence of (A7) and (A8), in the large-x limit $\exp(-2\tilde{x}\sqrt{1+q^2})\,\mathscr{L}_{U_j}[1+H_j^+]$ vanishes as well as $H_j^+ \times \exp[-2\tilde{x}\sqrt{1+q^2}]$ (according to (A3)) so that a_1 in (A4) proves to be zero. Then the definition (4.37) together with the choice (A2) enforce that a_0 is also equal to zero.

APPENDIX B

In the present appendix we study the structure of the ε-expansions of the functions H_U defined by the series representation (4.38).

B.1. Bounds for the H_{U_j}'s

According to integration properties, the linear operator $\mathscr{L}_U$ defined in (4.37) has the following properties,

$$|\mathscr{L}_U[f]| \leqslant \mathscr{L}_{|U|}[|f|] \tag{B1}$$

$$|U| < U' \Rightarrow \mathscr{L}_{|U|}[|f|] \leqslant \mathscr{L}_{U'}[|f|] \tag{B2}$$

and

$$0 \leqslant f \leqslant g \Rightarrow 0 \leqslant \mathscr{L}_{|U|}[f] \leqslant \mathscr{L}_{|U|}[g] \tag{B3}$$

Therefore, by a recurrence argument, the series representation (4.38) of H_U leads to the following result

$$\text{if} \quad |U| \leqslant U' \qquad \text{then} \quad |H_U| \leqslant H_{-U'} \tag{B4}$$

In the present appendix we will omit all irrelevant indices and coefficients and we consider only the prototype functions

$$U_1(\tilde{x}; \varepsilon) = e^{A_{\text{el}} \frac{\varepsilon}{2\tilde{x}}} - 1 \tag{B5}$$

and

$$U_2(\tilde{x}; \varepsilon; \tilde{b}) = e^{\varepsilon F(\tilde{x}; \varepsilon, \tilde{b})} - 1 \tag{B6}$$

where $F(\tilde{x}; \varepsilon, \tilde{b})$ is a continuous function of $\tilde{x}$ in the interval $\tilde{b} \leqslant \tilde{x} < +\infty$, which is bounded for all $\tilde{x} > \tilde{b}$ as follows,

$$|F(\tilde{x}; \varepsilon, \tilde{b})| \leqslant M_F(\varepsilon/\tilde{b})\, g(\tilde{x}) \tag{B7}$$

where $g(\tilde{x})$ is a continuous function integrable in the interval $[\tilde{b}, +\infty[$. Subsequently for all $\tilde{x} \geqslant \tilde{b}$

$$F(\tilde{x}; \varepsilon, \tilde{b}) \leqslant M_F(\varepsilon/\tilde{b})\, M_g(\tilde{b}) \equiv M_2(\varepsilon/\tilde{b}, \tilde{b}) \tag{B8}$$

where $M_g(\tilde{b})$ denotes the upper bound of g in the range $\tilde{b} \leqslant \tilde{x} < +\infty$.

Bounds upon the potentials U_j's are derived by noticing that for all reals v

$$\begin{cases} |e^{-|v|} - 1| \leqslant |v| \\ 0 \leqslant e^{|v|} - 1 \leqslant |v| e^{|v|} \end{cases} \tag{B9}$$

((B9) is a direct consequence of the series representation of the exponential.) (B9) implies that

$$|U_1(\tilde{x}; \varepsilon)| < U_1^{\max} \equiv \varepsilon_1 \frac{1}{\tilde{x}} \tag{B10}$$

where $\varepsilon_1 = \varepsilon M_1(\varepsilon/\tilde{b}, \Delta_{el})$ and

$$M_1(\varepsilon/\tilde{b}, \Delta_{el}) = \frac{\Delta_{el}}{2} \exp\left(\frac{\Delta_{el}}{2}\frac{\varepsilon}{\tilde{b}}\right) \quad \text{if} \quad \Delta_{el} > 0 \tag{B11a}$$

$$= \frac{|\Delta_{el}|}{2} \quad \text{if} \quad \Delta_{el} < 0 \tag{B11b}$$

Besides, if the sign of $F(\tilde{x})$ depends on $\tilde{x}$, $F(\tilde{x})$ may be written as $F(\tilde{x}) = F_+(\tilde{x}) - F_-(\tilde{x})$ with $F_+(\tilde{x}) = F(\tilde{x})$ if $F(\tilde{x}) > 0$ and $F_+(\tilde{x}) = 0$ otherwise, while $F_-(\tilde{x}) = -F(\tilde{x})$ if $F(\tilde{x}) < 0$ and $F_-(\tilde{x}) = 0$ otherwise. With these definitions $|F(\tilde{x})| = F_+(\tilde{x}) + F_-(\tilde{x})$. Using the decomposition

$$e^{\varepsilon F} - 1 = (e^{\varepsilon F_+} - 1)\, e^{-\varepsilon F_-} + (e^{-\varepsilon F_-} - 1) \tag{B12}$$

together with (B7) and (B9), we get

$$|U_2(\tilde{x}; \varepsilon, b)| \leqslant U_2^{\max} \equiv \varepsilon_2\, g(\tilde{x}) \tag{B13}$$

where $\varepsilon_2 = \varepsilon M_2(\varepsilon/\tilde{b}, \tilde{b})$ and

$$M_2(\varepsilon/\tilde{b}, \tilde{b}) = M_F(\varepsilon/\tilde{b}) \exp[\varepsilon M_F(\varepsilon/\tilde{b})\, M_g(\tilde{b})] \tag{B14}$$

The bounds (B10) and (B13) about the $\bar{U}_j$'s ensure that, according to (B4)

$$|H_{U_1}| \leqslant H_{-\varepsilon_1/t} \qquad \text{and} \qquad |H_{U_2}| \leqslant H_{-\varepsilon_2 g} \tag{B15}$$

As shown in the following, some information about the structure of the ε-expansions of the H_{U_j}'s can be derived from (B15). In particular in both cases, the linearity of integrals ensures that the nth term in the series (4.38) for $H_{-U_j^{\max}}$ is exactly of order ε_j^n, which is not the case when $U(\tilde{x}, \varepsilon)$ is not a linear function of ε.

B.2. ε-Expansions of Bounds for the H_{U_j}'s

First we consider $H_{-\varepsilon g}$. A mere integration by parts allows one to show that when $g(t)$ is positive, integrable at large t and continuous for $\tilde{b} \leqslant t < +\infty$,

$$\mathscr{L}_g[1](\tilde{x}) \leqslant \int_{\tilde{b}}^{+\infty} dt\, g(t) \equiv G(\tilde{b}) \tag{B16}$$

Since $\mathscr{L}_{-\varepsilon g}[1] = -\varepsilon \mathscr{L}_g[1]$, a recurrence argument proves that the nth term in the series representation (4.38) of $H_{-\varepsilon g}$ is a positive function of x which is

lower than $[\varepsilon G(\tilde{b})]^n$. Thus, $H_{-\varepsilon g}(\tilde{x})$ is lower than a geometric series which can be resummed with the result

$$H_{-\varepsilon g}(\tilde{x}) \leqslant \frac{\varepsilon G(\tilde{b})}{1-\varepsilon G(\tilde{b})} \tag{B17}$$

Therefore $H_{-\varepsilon g}(\tilde{x}; \varepsilon, \tilde{b})$ can be written as an ε-expansion whose coefficients are bounded functions of $\tilde{x}$,

$$H_{-\varepsilon g}(\tilde{x}) = \sum_{n=1}^{+\infty} \varepsilon^n G_n(\tilde{x}; \tilde{b}) \tag{B18}$$

with $G_n(\tilde{x}; \tilde{b}) \leqslant G_n(\tilde{b})$ for all $\tilde{x} \geqslant \tilde{b}$.

When $U(\tilde{x}) = \varepsilon/\tilde{x}$ the starting equation (A1) satisfied by H_U, is exactly solvable and the formal series (4.38) must coincide with the ε-expansion of the explicit exact solution. More precisely, $\exp(-x)[1+H_{\varepsilon/t}(x)]$ is a solution of the stationary radial Schroedinger equation for a quantum state with zero angular kinetic momentum and a negative energy -1, in the Coulomb potential $-\varepsilon/r$ in dimensionless units, and with boundary conditions (A2) and (A3). ((A2) is different from the corresponding condition in a Hydrogen atom.) The equation reads

$$\frac{d^2h}{d\tilde{x}^2} + \left[\frac{\varepsilon}{\tilde{x}} - 1\right] h = 0 \tag{B19}$$

The solutions of (B19) are well-known: with the boundary conditions (A2) and (A3)

$$1 + H_{\varepsilon/t}(\tilde{x}) = A(\varepsilon, \tilde{b})\, e^{\tilde{x}-\tilde{b}} W_{\varepsilon/2,\,1/2}(2\tilde{x}) \tag{B20}$$

where $A(\varepsilon, \tilde{b}) = [W_{\varepsilon/2,\,1/2}(2\tilde{b})]^{-1}$ and W is the Whittaker function. Up to a normalization factor

$$W_{\varepsilon/2,\,1/2}(2\tilde{x}) \propto (2\tilde{x})^{\varepsilon/2}\, e^{-\tilde{x}} \int_0^{+\infty} dt\, e^{-t} t^{-\varepsilon/2} \left[1 + \frac{t}{2\tilde{x}}\right]^{\varepsilon/2} \tag{B21}$$

The structure of the ε-expansion of $H_{\varepsilon/t}$ can be derived either from the ε-expansion of the above integral representation of $W_{\varepsilon/2,\,1/2}(2\tilde{x})$ or from the series representation (4.38). ((4.38) is also an ε-expansion of $H_{\varepsilon/t}$, since the nth term is exactly of order ε^n because of the linearity property of integration.) We choose to exhibit the second derivation in order to illustrate how the series representation provides information. A recurrence scheme using an

integration by parts and the fact that $\mathscr{L}_{1/t}[f(\gamma t);\gamma,\tilde{b}](\tilde{x}) = (1/\gamma)\,\mathscr{L}_{1/t}[f(t);1,\gamma\tilde{b}](\gamma\tilde{x})$ allows one to show a generalization of (A8) (with $\gamma = 2$),

$$\mathscr{L}_{1/t}[(\ln 2t)^p;2,\tilde{b}](\tilde{x}) = \frac{1}{2(p+1)}(\ln 2\tilde{x})^{p+1} + \sum_{n=1}^{p} A_{p,n}(\ln 2\tilde{x})^n + B_p(\tilde{x},\tilde{b}) \tag{B22}$$

where $B_p(\tilde{x},\tilde{b})$ is a bounded function of $\tilde{x}$ when $\tilde{x} > \tilde{b}$. Since the nth term in the series (4.38) for $U = \varepsilon/t$ is exactly proportional to ε^n, a recurrence scheme readily shows that the structure of the ε-expansion of $H_{\varepsilon/t}(\tilde{x})$ reads

$$H_{\varepsilon/t}(\tilde{x}) = \sum_{n=1}^{+\infty} \varepsilon^n \left[\frac{1}{n!}\left(\frac{\ln 2\tilde{x}}{2}\right)^n + b_{n-1}(\ln 2\tilde{x})^{n-1} + \cdots + b_1 \ln(2\tilde{x}) + B_n^*(\tilde{x},\tilde{b}) \right] \tag{B23}$$

In (B23) $B_n^*(\tilde{x},\tilde{b})$ is a function which is bounded for $\tilde{x} > \tilde{b}$. The coefficient at every order ε^n vanishes when $\tilde{x} = \tilde{b}$ (because $\mathscr{L}_{1/t}[f](\tilde{x} = \tilde{b}) = 0$). It diverges as $(1/n!)(\ln(2\tilde{x})/2)^n$ at large $\tilde{x}$ and the summation over the leading asymptotic behaviours at all orders in ε can be performed explicitly with the result

$$H_{\varepsilon/t}(\tilde{x}) \underset{\tilde{x}\to+\infty}{\sim} e^{\frac{\varepsilon}{2}\ln(2\tilde{x})} = (2\tilde{x})^{\varepsilon/2} \tag{B24}$$

The asymptotic behaviour (B24) indeed coincides with the leading large-distance behaviour of the explicit solution (B20) derived by using the integral representation (B21),

$$W_{\varepsilon/2,1/2}(2\tilde{x}) \underset{\tilde{x}\to+\infty}{\sim} (2\tilde{x})^{\varepsilon/2} e^{-\tilde{x}} \left[1 - \frac{\varepsilon(2+\varepsilon)}{8\tilde{x}} + \mathcal{O}\left(\frac{1}{\tilde{x}^2}\right) \right] \tag{B25}$$

B.3. Exact Solution at First Order in ε

First, the fact that the upper bounds $U_{\mathrm{j}}^{\max}(\tilde{x};\varepsilon_{\mathrm{j}},\tilde{b})$'s upon the U_{j}'s are of the form

$$U_{\mathrm{j}}^{\max}(\tilde{x};\varepsilon_{\mathrm{j}},\tilde{b}) = \varepsilon_{\mathrm{j}} V_{\mathrm{j}}^{\max}(\tilde{x}) \tag{B26}$$

(where ε_1 and ε_2 are defined in (B10) and (B13)) allows one to show that

$$H_{U_{\mathrm{j}}} = -\mathscr{L}_{U_{\mathrm{j}}}[1] + \sum_{n=2}^{+\infty} \varepsilon^n a_{\mathrm{j},n}(\tilde{x};\varepsilon,\tilde{b}) \tag{B27}$$

with for all $\tilde{x} \geqslant \tilde{b}$,

$$|a_{j,n}(\tilde{x}; \varepsilon, \tilde{b})| \leqslant [M_j(\varepsilon/\tilde{b}, \tilde{b}^{j-1})]^n A_{j,n}(\tilde{x}, \tilde{b}) \tag{B28}$$

where the M_j's are defined in (B11) and (B14). In (B28) $A_{1,n}(\tilde{x}; \tilde{b})$ does not diverge faster than $(\ln \tilde{x})^n$ when $\tilde{x}$ goes to infinity, while $A_{2,n}(\tilde{x}; \tilde{b})$ is a bounded function of $\tilde{x}$ for all $\tilde{x} \geqslant \tilde{b}$. The demonstration is the following. According to the series representation (4.38) for H_{U_j}, the inequalities (B1) and (B2) together with the proportionality relation (B26) lead to

$$|H_{U_j} + \mathscr{L}_{U_j}[1]| \leqslant \sum_{n=2}^{+\infty} \varepsilon_j^n \mathscr{L}_{V_j^{\max}}[\mathscr{L}_{V_j^{\max}} \cdots [\mathscr{L}_{V_j^{\max}}[1]] \cdots] \tag{B29}$$

where the coefficient of ε_j^n contains n operators $\mathscr{L}_{V_j^{\max}}$. (B29) implies that the sum in (B27) indeed starts at the order ε^2. Moreover, according to (4.38), the right term in (B29) may be written as

$$[H_{-U_j^{\max}} + \mathscr{L}_{-U_j^{\max}}[1]] \tag{B30}$$

The explicit structures of the ε_j-expansions (B18) and (B23) for the $H_{-U_j^{\max}}$'s together with the results (A8) and (B16) for $\mathscr{L}_{-U_j^{\max}}$ imply that

$$|H_{U_j} + \mathscr{L}_{U_j}[1]| \leqslant \sum_{n=2}^{+\infty} \varepsilon_j^n A_{j,n}(\tilde{x}; \tilde{b}) \tag{B31}$$

where the $A_{j,n}$ have the properties given after (B28).

Second, we show that the ε-expansion of $\mathscr{L}_{U_j}[1] - \mathscr{L}_{U_j^{\text{lin}}}[1]$ starts at order ε^2, where the linearized potential U_j^{lin} is the first-order term in the expansion of the exponential involved in the definitions (B5) and (B6) of the U_j's. More precisely

$$\mathscr{L}_{U_j}[1] = \mathscr{L}_{U_j^{\text{lin}}}[1] + \varepsilon^2 R_{L_j}(\tilde{x}; \varepsilon, \tilde{b}) \tag{B32}$$

where for all $\tilde{x} \geqslant \tilde{b}$, R_{L_j} is a bounded function of $\tilde{x}$ and the dependence of its bound $M_{L_j}(\varepsilon/\tilde{b}, \tilde{b})$ upon ε is entirely contained in $M_1(\varepsilon/b)$ if $j = 1$ or in $[M_F(\varepsilon/\tilde{b})]^2 \exp[\varepsilon M_F(\varepsilon/\tilde{b})\, M_g(\tilde{b})]$ if $j = 2$. (B32) is derived as follows. First we notice that

$$\mathscr{L}_{U_j}[1] - \mathscr{L}_{U_j^{\text{lin}}}[1] = \mathscr{L}_{U_j - U_j^{\text{lin}}}[1] \tag{B33}$$

Moreover for all reals v

$$\begin{cases} |e^{-|v|} - 1 + |v|| \leqslant v^2 \\ e^{|v|} - 1 - |v| \leqslant v^2 e^{|v|} \end{cases} \tag{B34}$$

so that

$$|U_1(\tilde{x}; \varepsilon) - U_1^{\text{lin}}(\tilde{x}; \varepsilon)| \leqslant \frac{|\Delta_{\text{el}}|}{2} M_1(\varepsilon/\tilde{b})\, \varepsilon^2 \frac{1}{x^2} \tag{B35}$$

A decomposition similar to (B12) reads

$$\begin{aligned} e^{\varepsilon F} - 1 - \varepsilon F = (e^{\varepsilon F_+} - 1 - \varepsilon F_+)\, e^{-\varepsilon F_-} + \varepsilon F_+ (e^{-\varepsilon F_-} - 1) \\ + (e^{-\varepsilon F_-} - 1 + \varepsilon F_-) \end{aligned} \tag{B36}$$

and we get

$$|U_2(\tilde{x}; \varepsilon) - U_2^{\text{lin}}(\tilde{x}; \varepsilon)| \leqslant M_F(\varepsilon/\tilde{b})\, M_2(\varepsilon/\tilde{b}, \tilde{b})\, \varepsilon^2 g^2(\tilde{x}) \tag{B37}$$

According to (B2), the latter bounds together with (B33) imply that

$$|\mathscr{L}_{U_j}[1] - \mathscr{L}_{U_j^{\text{lin}}}[1]| \leqslant \varepsilon^2 \mathscr{L}_{g_j}[1] \tag{B38}$$

where $g_1(\tilde{x}) = (|\Delta_{\text{el}}|/2)\, M_1(\varepsilon/\tilde{b})\, 1/x^2$ and $g_2(\tilde{x}) = M_F(\varepsilon/\tilde{b})\, M_2(\varepsilon/\tilde{b}, \tilde{b})\, g(\tilde{x})^2$. Since $1/\tilde{x}^2$ as well as $g(\tilde{x})^2$ are continuous for $\tilde{x} \geqslant \tilde{b}$ and integrable when $\tilde{x}$ goes to ∞, the result (B16) can be applied to the g_j's and leads to (B32).

Subsequently, according to (B27) and (B32)

$$H_{U_j}(\tilde{x}) = -\mathscr{L}_{U_j^{\text{lin}}}[1](\tilde{x}) + \varepsilon^2 R_{U_j}(\tilde{x}; \varepsilon, \tilde{b}) \tag{B39}$$

where if $\varepsilon/\tilde{b}$ and $\tilde{b}$ are kept bounded, $\lim_{\varepsilon \to 0} R_{U_j}(\tilde{x}, \varepsilon, \tilde{b}) < +\infty$ and $R_{U_j}(\tilde{x}, \varepsilon, \tilde{b})$ does not diverge faster than $\tilde{x}^{p(\varepsilon)}$ with $\lim_{\varepsilon \to 0} p(\varepsilon) = 0$ when $\tilde{x}$ goes to $+\infty$. We recall that the result (B39) holds for a potential $U_j(\tilde{x}; \varepsilon)$ which may be not bounded for all $\tilde{x} \geqslant 0$. The only hypotheses about $U_j(\tilde{x}; \varepsilon)$ are that $U_j(\tilde{x}; \varepsilon)$ tends to zero at least as fast as $\varepsilon/\tilde{x}$ when $\tilde{x}$ becomes larger than 1. The property (B39) can be applied to U_j^{lin} and we get

$$H_{U_j}(\tilde{x}) - H_{U_j^{\text{lin}}}(\tilde{x}) = \varepsilon^2 [R_{U_j}(\tilde{x}; \varepsilon, \tilde{b}) - R_{U_j^{\text{lin}}}(\tilde{x}; \varepsilon, \tilde{b})] \tag{B40}$$

The solutions of the homogeneous equations (A1) for U_j and U_j^{lin} respectively coincide only at the first order in their ε-expansions.

REFERENCES

1. A. Alastuey, F. Cornu, and A. Perez, Virial expansions for quantum plasmas: Diagrammatic resummations, *Phys. Rev. E* **49**:1077 (1994).
2. F. Cornu, Correlations in quantum plasmas, I. Resummations in Mayer-like diagrammatics, *Phys. Rev. E* **53**:4562 (1996).
3. F. Cornu, Quantum plasmas with or without a uniform field. II. Exact low-density free energy, *Phys. Rev. E* **58**:5293 (1998).
4. R. L. Guernsey, Correlation effects in semi-infinite plasmas, *Phys. Fluids* **13**:2089 (1970).
5. E. Haga, On Mayer's theory of dilute ionic solutions, *J. of the Physical Society of Japan* **8**:714 (1953).
6. J. P. Hansen and I. R. Mac Donalds, *Theory of Simple Liquids* (Academic Press, London, 1986).
7. J. D. Jackson, *Classical Electrodynamics* (Wiley, New York, 1962).
8. B. Jancovici, Classical Coulomb systems near a plane wall. I. *J. Stat. Phys.* **28**:43 (1982).
9. L. D. Landau and E. M. Lifshitz, *Course of Theoretical Physics. Electrodynamics of Continuous Media*, Vol. 8 (Pergamon Press, Oxford, 1985).
10. E. Lieb and J. L. Lebowitz, The constitution of matter: Existence of thermodynamics for systems composed of electrons and nuclei, *Adv. Math.* **9**:316 (1972).
11. E. Meeron, Theory of potentials of average force and radial distribution functions in ionic solutions, *J. Chem. Phys.* **28**:630 (1958).
12. A. Messiah, *Quantum Mechanics* (Wiley, New York, 1958).
13. A. S. Usenko and I. P. Yakimenko, Interaction energy of stationary charges in a bonded plasma, *Sov. Techn. Phys. Lett.* **5**:549 (1979).
14. D. Zwillinger, *Handbook of Differential Equations* (Academic Press, 1989).